Journal of Statistical Physics, Vol. 84, Nos. 5/6, 1996

Local Second-Order Boundary Methods for Lattice Boltzmann Models

I. Ginzbourg[1] and D. d'Humières[2]

Received August 2, 1995

A new way to implement solid obstacles in lattice Boltzmann models is presented. The unknown populations at the boundary nodes are derived from the locally known populations with the help of a second-order Chapman–Enskog expansion and Dirichlet boundary conditions with a given momentum. Steady flows near a flat wall, arbitrarily inclined with respect to the lattice links, are then obtained with a third-order error. In particular, Couette and Poiseuille flows are exactly recovered without the Knudsen layers produced for inclined walls by the bounce back condition.

KEY WORDS: Lattice Boltzmann equation; boundary conditions; Chapman–Enskog expansion; Knudsen layer.

1. INTRODUCTION

Lattice-gas[1] and lattice Boltzmann models[2, 3] have been introduced during the past 10 years as alternative ways to simulate fluid flows. They are respectively simplified molecular-dynamics or Boltzmann equations, restricted to regular lattices and limited sets of velocities. Further information about theory and applications of these models can be found in two extensive reviews: ref. 4 for lattice-gas models and ref. 5 for lattice Boltzmann models.

As in molecular-dynamics or Boltzmann equations, the macroscopic fields (pressure, velocity,...) are not handled explicitly in lattice-gas or

[1] CNRS, Applications Scientifiques du Calcul Intensif, Université Paris Sud, 91405, Orsay Cedex, France; e-mail: ginsburg@asci.fr.

[2] CNRS and Université Pierre et Marie Curie, Laboratoire de Physique Statistique de l'ENS, 75231 Paris Cedex 05, France; e-mail: dominiq@physique.end.fr.

0022-4715/96/0900-0927$09.50/0

lattice Boltzmann models, but are computed *a posteriori* from the local particle populations. Consequently, boundary conditions are implemented implicitly by supplying the unknown populations coming from outside the fluid; i.e., each boundary condition, such as solid walls, inlet, outlets,..., requires the knowledge of an appropriate closure relation for these unknown populations.

The most commonly used condition to implement solid walls is the so-called *bounceback rule*, where the populations leaving the fluid return to the node of departure with the opposite velocity. This rule is not only very simple, but also enforces mass conservation in the computational domain. Indeed, this implicit annihilation of the velocity raises the question of the exact location of the no-slip walls. This problem becomes especially important for effective simulations of flows when the distance between walls can be of the order of a few lattice units and hence accurate location of solid walls with respect to the lattice is crucial. Examples of such flows can be found in porous media[6–9] or due to the motion of Solid particles in Suspension.[10–13]

When the bounceback rule is applied, linear analysis[14] of stationary flows invariant by translation along the wall locates no-slip walls exactly halfway between the boundary fluid nodes and the next ones inside the solid. Since this analysis is based on a first-order Chapman–Enskog expansion, it gives an exact location of no-slip walls for linear flows only. A second-order analysis of this problem[15–17] has shown that the actual position of the no-slip walls depends also on the size of computational domain, the kinematic viscosity, and one of the eigenvalues of the collision matrix unrelated to any physical parameter of the simulated flow. For Poiseuille flows parallel to one of the population velocities, this second-order analysis specifies exactly the distance between no-slip walls and boundary nodes, either with the bounceback rule for some eigenvalues of the collision matrix[15, 16] or for some mixing of bounceback and specular reflections.[17]

Unlike the above methods in which the unknown incoming populations are computed from the known outgoing ones, some authors have proposed alternative methods in which these unknown populations are directly computed from Dirichlet boundary conditions (known velocities on the solid wall). In the approaches proposed by Ziegler[18] and Noble *et al.*[19] for walls parallel to a link of the FHP lattice, the boundary conditions enforce prescribed velocities on the boundary nodes. It turns out that Ziegler's method is a special case of a mixture of bounceback and specular reflections, for which the first-order Chapman–Enskog expansion locates the wall on the boundary nodes. However, this method has the same limitation as the bounceback rule: the position of the solid wall is exact for Couette flows only. The second method provides second-order accuracy

but seems difficult to extend when the wall is no longer located on nodes (inclined walls) or when the number of unknown populations is larger than the number of velocity components.

Skordos[20] and Ginzbourg[17] have proposed more general methods in which the unknown populations are computed from first-order[20] or second-order[17] Chapman–Enskog expansions, the derivatives being approximated by a finite-difference scheme. In Skordos' method the pressure (or the density) is assumed to be known at the solid. In Ginzbourg's method the density is kept unknown and the unknown populations are obtained as solutions of a linear system derived from the second-order Chapman–Enskog expansion. Since finite-difference approximations of derivatives are used in these methods, they require access to the populations of the neighboring lattice nodes, and thus they are in general nonlocal. The introduction of finite differences into lattice Boltzmann models also makes these methods noticeably less stable.

Moreover, Knudsen-type layers appear near the walls when they are inkclined with respect to lattice links and bounceback or a combination of bounceback and specular reflections are used, as shown in this paper. This problem seems difficult to solve on regular lattices when finite difference approximations are used, since they assume that Dirichlet conditions are imposed on some set of points obtained from the discretization of the inclined solid wall rather than on the real wall itself.

In this paper we introduce a new boundary approach, referred as the *local second-order boundary* (LSOB) method, which does not use finite differences, but computes locally at each boundary node all the derivatives necessary for the second-order expansion of the unknown populations from the known ones. The main idea of this method is to split the hydrodynamic fields–momentum, its first- and second-order derivatives, and density–into two sets: the known fields given by the boundary conditions and the unknown fields. The linear system relating these unknown fields to the known populations is then written at each boundary node using two kinds of known populations: those arriving from neighboring liquid nodes and those which should leave it and propagate into the solid. It follows that the number of known populations is equal to the number of velocities defining the lattice Boltzmann model. We will show that this number is always larger than the number of unknown hydrodynamic fields, at least for Dirichlet conditions. At this stage the difficulty is to show that the problem is numerically well posed, i.e., that a subset of linear equations can be extracted in order to obtain an invertible linear system. Assuming this critical step successfully solved, the unknown boundary populations arriving from the solid are then obtained as linear combinations of a subset of the known populations at this node. The coefficients of these combinations

depend upon the inclination of the solid wall, its velocity, the distance between the wall and the boundary node, and the eigenvalues of the collision matrix. For a fixed wall with a general Dirichlet condition, these coefficients are computed only once at each boundary node during the initialization procedure and they are then used during the usual iteration steps.

With the LSOB method Dirichlet conditions on arbitrary smooth walls, such as planes, spheres, cylinders,..., can be introduced into steady 3D flows with a third-order error. In particular, Couette and Poiseuille flows can be simulated exactly for any inclined channels of an arbitrary small width. Thus, the method solves with a third-order error both problems: location of no-slip walls and appearance of nonhydrodynamic solutions. In principle, this method can be extended to walls moving with a velocity very small compared to the particle velocities. In this case the closure systems at the boundary nodes have to be recomputed each time the wall is moved, with potential difficulties when the wall crosses the lattice nodes.

Thus, the paper is organized as follows. Section 2 is devoted to a general exposition of the method within the following framework: the 3D flow is assumed to be stationary and the fluid domain is bounded by an infinite flat solid wall, arbitrarily inclined with respect to the lattice axes, with given Dirichlet conditions. Although the method applies to lattice Boltzmann models on triangular FHP and facecentered hypercubic (FCHC) lattices, the symbolic derivation will be given for the FCHC model only. For simplicity the technical details are worked out only for a flat wall kept parallel to one axis of the lattice and are given in section 3. The extension of the results to more general cases, such as smooth surfaces, is almost straightforwardy but requires cumbersome formulas which cannot be easily given within the scope of this paper.

These results are applied to some particular flows in section 3 and in Appendix A. The numerical results are compared to those obtained by the bounceback rule. They show that the new method gives the exact solutions and removes the nonhydrodynamic modes produced by the bounceback condition when the velocity field can be written as a second-order polynomial in space coordinates.

Two difficult questions raised by this new method are briefly studied in Appendices A and B. In Appendix A we show that the total mass is automatically conserved by LSOB methods when stationary Couette or Poiseuille flows are simulated in inclined channels. The derivation is only given for a simplified discretization of the wall. The linear stability analysis of the lattice Boltzmann method with the new boundary conditions is given in Appendix B for a very simple geometry.

2. GENERAL FRAMEWORK OF THE LOCAL SECOND-ORDER BOUNDARY METHOD

2.1. Lattice Boltzmann Equation and Second-Order Chapman–Enskog Expansion

In this paper, we will consider the standard lattice Boltzmann equation[2, 3] in which the nonlinear terms in the equilibrium distribution are neglected [see relation (6)]. For the lattice nodes $\mathbf{r}$ surrounded by the liquid fraction of the medium, the lattice Boltzmann equation with an external force $\mathbf{F}$ is given by

$$N_i(\mathbf{r}+\mathbf{C}_i, t+1) = N_i(\mathbf{r}, t) + \sum_{j=1}^{b_m} \mathscr{A}_{ij} N_j(\mathbf{r}, t) + d'\rho(\mathbf{r}, t)\,\mathbf{F}\cdot\mathbf{C}_i, \quad i \in \{1,..., b_m\} \tag{1}$$

where N_i is the population moving with velocity $\mathbf{C}_i$, $\mathscr{A}$ is the collision matrix, and d' is a model-dependent parameter given in relation (10).

Density ρ and momentum $\mathbf{j}$ are defined in the standard way

$$\rho(\mathbf{r}, t) = \sum_{i=1}^{b_m} N_i(\mathbf{r}, t) \tag{2}$$

$$\mathbf{j}(\mathbf{r}, t) = \sum_{i=1}^{b_m} N_i(\mathbf{r}, t)\,\mathbf{C}_i \tag{3}$$

Their conservation is imposed on the collision matrix $\mathscr{A}$ by

$$\mathscr{A}\cdot\mathbf{1} = \mathscr{A}\cdot\mathbf{C}_\alpha = 0, \qquad \forall\alpha \in \{1,..., D\} \tag{4}$$

where D is the dimension of the physical space, $\mathbf{1}$ is the b_m-vector $\{1,..., 1\}$, and the vector $\mathbf{C}_\alpha$ is built from the components of the b_m population velocities in direction α. The collision matrix is fully defined by the choice of its nonzero eigenvalues and the corresponding eigenvectors. These eigenvectors are given for FHP models in ref. 14 (see also Appendix B) and for FCHC models in refs. 17 and 21. The relation between the eigenvalues and the coefficients of the usual collision matrix can be found in ref. 22. Note that the term $N_j - N_j^{\text{eq}}$ is replaced by N_j in the collision operator $\sum \mathscr{A}_{ij} N_j$ since the nonlinear terms in the equilibrium distribution N_j^{eq} are neglected.

When the ratio ε between the lattice unit and a characteristic length of the medium is smaller than one, the second-order Chapman–Enskog

expansion gives the following approximation for any solution of the lattice Boltzmann equation (1):

$$N_i(\mathbf{r}, t) = N_i^{(\mathrm{eq})}(\mathbf{r}, t) + N_i^{(1)}(\mathbf{r}, t) + O(\varepsilon^3), \qquad i \in \{1, \ldots, b_m\} \tag{5}$$

where $N_i^{(\mathrm{eq})}$ is a function of the local conserved quantities, $N_i^{(1)}$ is $O(\varepsilon)$, and thus a function of the first derivatives of these quantities, and $N_i^{(2)}$ is $O(\varepsilon^2)$, and thus a function of their second derivatives. The first two terms in the right hand side of (5) are isotropic for the FHP and FCHC lattices and have the same expression for any Cartesian coordinate system. This is no longer true for the second-order term $N_i^{(2)}$ which is anisotropic. In the sequel, the Cartesian coordinate system $\{x, y\}$ or $\{x, y, z\}$ is chosen along "lattice axes," i.e., such that one velocity is written (1, 0) for FHP models and three velocities are written (1, 0, 0), (0, 1, 0), and (0, 0, 1) for the 3D projection of FCHC models.

Such second-order Chapman–Enskog expansions can be found in ref. 23 for the FHP model and steady flows, and in ref. 16 for FCHC models with rest populations and time-dependent flows. For steady flows and for both FHP and FCHC models without rest populations, the different orders are given by

$$N_i^{(\mathrm{eq})}(\mathbf{r}, t) = d(\mathbf{r}, t) + d'\mathbf{j} \cdot \mathbf{C}_i + O(\|\mathbf{j}^2\|) \tag{6}$$

$$N_i^{(1)}(\mathbf{r}, t) = \frac{d'}{\lambda_\psi} \sum_{\alpha, \beta} \frac{\partial j_\alpha}{\partial \beta} Q_{i\alpha\beta} \tag{7}$$

$$N_i^{(2)}(\mathbf{r}, t) = d' \frac{\nu}{\lambda_2} \sum_{\alpha \neq \beta} \left[\frac{\partial^2 j_\alpha}{\partial \beta^2} + \ell' \frac{\partial^2 j_\beta}{\partial \alpha \, \partial \beta} \right] T_{i\alpha\beta\beta}, \qquad \ell' = \begin{cases} 3, & \text{FHP} \\ 2, & \text{FCHC} \end{cases} \tag{8}$$

where α and β are taken in $\{x, y\}$ or $\{x, y, z\}$, c^2 is the square of population velocities, the density per cell d is given by

$$d(\mathbf{r}, t) = \frac{\rho(\mathbf{r}, t)}{b_m} \tag{9}$$

and the model's parameter d' is given by

$$d' = \frac{D}{c^2 b_m}, \qquad D = \begin{cases} 2, & \text{FHP} \\ 4, & \text{FCHC} \end{cases} \tag{10}$$

The first-order eigenvectors of the collision matrix, associated with the eigenvalue λ_ψ, are

$$Q_{i\alpha\beta} = C_{i\alpha} C_{i\beta} - \frac{c^2}{D} \delta_{\alpha\beta}, \qquad \forall \alpha, \beta \tag{11}$$

and the second-order eigenvectors of the collision matrix, associated with the eigenvalue λ_2, are

$$T_{i\alpha\beta\beta} = C_{i\alpha} - \frac{D+2}{c^2} C_{i\alpha} C_{i\beta}^2, \qquad \forall \alpha \neq \beta \tag{12}$$

Hereafter, the FCHC lattice is assumed; the implementation of the new boundary technique for the FHP lattice can be derived in a similar way (an example can be found in Appendix B).

2.2. Generalized Boundary Conditions

When there are no solid walls, all populations are defined by the lattice Boltzmann equation (1). When solid walls are introduced, *boundary nodes* $\mathbf{z}_0$ appear, for which the populations can be divided in two nonempty subsets: known *local* populations N_i^{loc} which arrive from the neighboring fluid nodes, and *unknown* incoming populations N_i^{in} which should arrive from the "solid" node $\mathbf{z}_0 - \mathbf{C}_i$ (see Fig. 1). Let $I_i^{\text{loc}}(\mathbf{z}_0)$ and $I_i^{\text{in}}(\mathbf{z}_0)$ be the

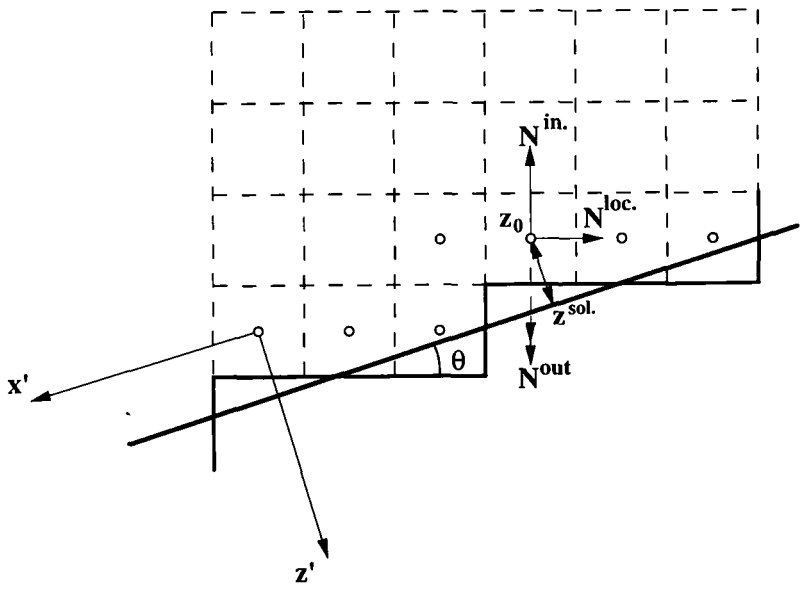

Fig. 1. x–z section of the FCHC lattice for a solid wall parallel to the y axis.

subsets of indices i for the populations $I_i^{\text{loc}}(\mathbf{z}_0)$ and $I_i^{\text{in}}(\mathbf{z}_0)$, respectively, with

$$\begin{aligned} I_i^{\text{loc}}(z_0) \cup I^{\text{in}}(\mathbf{z}_0) &= \{1,\ldots, b_m\} \\ I_i^{\text{loc}}(z_0) \cup I^{\text{in}}(\mathbf{z}_0) &= \{\varnothing\} \end{aligned} \tag{13}$$

Let L^{loc} be the number of local populations N_i^{loc} and L^{in} the number of unknown populations N_i^{in} in the node $\mathbf{z}_0 (L^{\text{loc}} + L^{\text{in}} = b_m)$.

In addition, to each unknown population $N_i^{\text{in}}(\mathbf{z}_0)$, there corresponds a known one $N_i^{\text{out}}(\mathbf{z}_0)$ leaving the lattice with an opposite velocity:

$$\mathbf{C}_j = -\mathbf{C}_i, \qquad i \in I^{\text{in}}(\mathbf{z}_0), \quad j \in I^{\text{out}}(\mathbf{z}_0) \tag{14}$$

Note that $N_i^{\text{out}}(\mathbf{z}_0)$, defined for $i \in I^{\text{out}}(\mathbf{z}_0)$, is the postcollision population given by the right-hand term of (1), while $N^{\text{loc}}(\mathbf{z}_0)$ is the post-propagation population. Let L^{out} be the number of leaving populations N_i^{out} in the node $\mathbf{z}_0 (L^{\text{out}} = L^{\text{in}}$ and $L^{\text{loc}} + L^{\text{out}} = b_m)$.

The goal of a generalized boundary condition is to compute the L^{in} unknown populations N_i^{in}, in the node $\mathbf{z}_0$ in such a way that some given conditions, for instance, a given value J^{sol} of the momentum, would be imposed on a given boundary surface with a third-order error $O(\varepsilon^3)$. A systematic way to achieve this goal is to compute all the unknown quantities appearing in the different terms (6)–(8) of the second-order Chapman–Enskog expansion (5) as linear functions of the b_m known populations N_i^{loc} and N_i^{out} fulfilling all the boundary constraints with the prescribed accuracy. If this linear problem can be successfully solved, the unknown populations are obtained as linear functions of the known ones:

$$\begin{aligned} N_i^{\text{in}}(\mathbf{z}_0) = {} & d(\mathbf{z}_0) + d' \mathbf{j}^{\text{sol}} \cdot \mathbf{C}_i \\ & + \sum_{j \in I^{\text{loc}}} P_{ij}(\mathbf{z}_0) \{ N_j^{\text{loc}}(\mathbf{z}_0) - d' \mathbf{j}^{\text{sol}} \cdot \mathbf{C}_j \} \\ & + \sum_{j \in I^{\text{out}}} P_{ij}(\mathbf{z}_0) \{ N_j^{\text{out}}(\mathbf{z}_0) - d(\mathbf{z}_0) - d' (\mathbf{j}^{\text{sol}} + \rho \mathbf{F}) \cdot \mathbf{C}_j \}, \quad i \in I^{\text{in}}(\mathbf{z}_0) \end{aligned} \tag{15}$$

where the local density is kept unknown and its value must be automatically supplied by the algorithm along with the matrix $\mathbf{P}(\mathbf{z}_0) = (P_{ij}(\mathbf{z}_0))$.

The existence of such an algorithm is not obvious *a priori* for general boundary conditions and surfaces. In this paper we exhibit an algorithm for a Dirichlet boundary condition on an infinite flat wall parallel to a fourfold symmetry axis of the 3D FCHC lattice. Several parts of the derivation are kept in their most general form, allowing the results to be extended

in a rather straightforward manner to more general orientations of flat walls, to smooth surfaces, or to different boundary conditions, at the expense of a slightly more complicated algebra. The extension of the method to the difficult problem of surfaces with sharp edges, such as a corner between two planes, is left for future work.

2.3. Unknown Derivatives on a Flat Wall

Inspecting the terms (6)–(8) entering the second-order Chapman–Enskog expansion, one sees that they may involve up to twenty five unknown quantities the 3 components of the momentum, their 9 first-order derivatives, 12 of their 18 second-order derivatives, and the density. This number of unknowns is larger than the number of known populations, 18 for the 3D FCHC lattice, and they cannot be extracted from $N_i^{\text{loc}}(\mathbf{z}_0)$ and $N_i^{\text{out}}(\mathbf{z}_0)$ without further information. Indeed this information must be sought from the boundary conditions; for instance, Dirichlet boundary conditions on a smooth wall provide, everywhere on this wall, not only the velocity components, but also all their derivatives along any directions tangent to the wall. In order to keep the algebra as simple as possible, in this paper the method will be given explicitly for the Dirichlet boundary condition with a uniform momentum $\mathbf{J}^{\text{sol}}$ on a flat wall.

Let $\{x', y', z'\}$ denote the orthogonal coordinate system associated with the flat wall: the z'-axis is perpendicular to the wall, its positive unit vector $\mathbf{n}$ being directed outward from the fluid; the x' and y' axes are parallel to the wall (see Fig. 1). For any boundary lattice node $\mathbf{z}_0$ appearing from the discretization of the solid wall, let $\mathbf{z}_0^{\text{sol}}$ be its orthogonal projection on the wall and $\delta(\mathbf{z}_0)$ its algebraic distance from $\mathbf{z}_0$:

$$\delta(\mathbf{z}_0) = (\mathbf{z}_0 - \mathbf{z}_0^{\text{sol}}) \cdot \mathbf{n} \tag{16}$$

With these notations and a uniform momentum on the flat wall, the first- and second-order derivatives of the momentum along x' and y' are exactly equal to zero everywhere on the wall, and consequently at the points $\mathbf{z}_0^{\text{sol}}$:

$$\begin{aligned} &\frac{\partial j_{\alpha'}}{\partial x'}(\mathbf{z}_0^{\text{sol}}) = \frac{\partial j_{\alpha'}}{\partial y'}(\mathbf{z}_0^{\text{sol}}) = 0 \\ &\frac{\partial^2 j_{\alpha'}}{\partial x'^2}(\mathbf{z}_0^{\text{sol}}) = \frac{\partial^2 j_{\alpha'}}{\partial x' y'}(\mathbf{z}_0^{\text{sol}}) = \frac{\partial^2 j_{\alpha'}}{\partial y'^2}(\mathbf{z}_0^{\text{sol}}) = 0, \qquad \alpha' = \{x', y', z'\} \end{aligned} \tag{17}$$

A further reduction of the number of unknown derivatives comes from the continuity equation for steady flows

$$\frac{\partial j_{z'}}{\partial z'} = -\left(\frac{\partial j_{x'}}{\partial x'} + \frac{\partial j_{y'}}{\partial y'}\right) \tag{18}$$

and its derivatives along the three axes

$$\frac{\partial^2 j_{z'}}{\partial \alpha' \, \partial z'} = -\left(\frac{\partial^2 j_{x'}}{\partial \alpha' \, \partial x'} + \frac{\partial^2 j_{y'}}{\partial \alpha' \, \partial y'}\right), \qquad \alpha' \in \{x', y', z'\} \tag{19}$$

Thus only two first-order and six second-order derivatives of the momentum are nonzero and unknown on a flat wall with a uniform momentum. For the subsequent developmlent, it is convenient to write these derivatives times d' as the components of a general unknown vector $\mathbf{X}(\mathbf{z}_0)$:

$$\mathbf{X}(\mathbf{z}_0) = d'\left(\frac{\partial j_{x'}}{\partial z'}, \frac{\partial j_{y'}}{\partial z'}, \frac{\partial^2 j_{x'}}{\partial z'^2}, \frac{\partial^2 j_{x'}}{\partial x' \, \partial z'}, \frac{\partial^2 j_{y'}}{\partial z'^2}, \frac{\partial^2 j_{y'}}{\partial y' \, \partial z'}, \frac{\partial^2 j_{x'}}{\partial y' \, \partial z'}, \frac{\partial^2 j_{y'}}{\partial x' \, \partial z'}\right)(\mathbf{z}_0^{\mathrm{sol}}) \tag{20}$$

Assuming δ of the order of a few lattice units, i.e., of order ε, the momentum and its first- and second-order derivatives on $\mathbf{z}_0$ can now be obtained from the following Taylor expansions:

$$j_{\alpha'}(\mathbf{z}_0) = j_{\alpha'}^{\mathrm{sol}} + \delta \frac{\partial j_{\alpha'}}{\partial z'}(\mathbf{z}_0^{\mathrm{sol}}) + \frac{1}{2}\delta^2 \frac{\partial^2 j_{\alpha'}}{\partial z'^2}(\mathbf{z}_0^{\mathrm{sol}}) + O(\varepsilon^3), \quad \alpha' = \{x', y', z'\} \tag{21}$$

$$\begin{aligned}
&\frac{\partial j_{\alpha'}}{\partial z'}(\mathbf{z}_0) = \frac{\partial j_{\alpha'}}{\partial z'}(\mathbf{z}_0^{\mathrm{sol}}) + \delta \frac{\partial^2 j_{\alpha'}}{\partial z'^2}(\mathbf{z}_0^{\mathrm{sol}}) + O(\varepsilon^3), \qquad \alpha' = \{x', y'\} \\
&\frac{\partial j_{z'}}{\partial z'}(\mathbf{z}_0) = \delta \frac{\partial^2 j_{z'}}{\partial z'^2}(\mathbf{z}_0^{\mathrm{sol}}) + O(\varepsilon^3) \\
&\frac{\partial j_{\alpha'}}{\partial \beta'}(\mathbf{z}_0) = \delta \frac{\partial^2 j_{\alpha'}}{\partial \beta' \, \partial z'}(\mathbf{z}_0^{\mathrm{sol}}) + O(\varepsilon^3), \qquad \{\alpha', \beta'\} = \{x', y'\} \\
&\frac{\partial j_{z'}}{\partial \beta'}(\mathbf{z}_0) = O(\varepsilon^3), \qquad \{\alpha', \beta'\} = \{x', y'\}
\end{aligned} \tag{22}$$

and

$$\frac{\partial^2 j_{\alpha'}}{\partial \beta' \, \partial z'}(\mathbf{z}_0) = \frac{\partial^2 j_{\alpha'}}{\partial \beta' \, \partial z'}(\mathbf{z}_0^{\mathrm{sol}}) + O(\varepsilon^3), \quad \alpha' = \{x', y'\}, \quad \beta' = \{x', y', z'\} \tag{23}$$

the other second-order derivatives being of $O(\varepsilon^3)$.

Then the momentum at the boundary node $\mathbf{z}_0$ and its first and second derivatives can be expressed with a third-order error as linear combinations of eight momentum derivatives on the wall. A first strategy, worked out explicitly in the next subsections, is to consider the vector $\mathbf{X}$ and the local cell density $d(\mathbf{z}_0)$ as the only unknowns of the problem. In Appendix A, using Couette and Poiseuille flows as examples, a second strategy is given in which the Taylor expansion is used for the momentum only and starts from the boundary node $\mathbf{z}_0$; the number of unknown second-order derivatives on $\mathbf{z}_0$ is kept equal to six using (23) and it can be shown. with the help of a symmetry argument, the continuity equation, and relations (22), that there are only five unknown quantities entering the first-order term of the Chapman–Enskog expansion:

$$\left\{\frac{\partial j'_x}{\partial x'}, \frac{\partial j'_x}{\partial z'}, \frac{\partial j'_y}{\partial y'}, \frac{\partial j'_y}{\partial z'}, \frac{\partial j'_x}{\partial y'} + \frac{\partial j'_y}{\partial x'}\right\}(\mathbf{z}_0) \tag{24}$$

This second form of the problem requires more known populations to find a solution and may be difficult to use in some complex geometry. However, in some situations, it gives simpler formulas for which the analytical calculations can be pushed farther than with the first approach.

2.4. Second-Order Approximation near a Flat Solid Wall

Let the $\mathbf{C}'_i$ be the population velocities expressed in the inclined coordinate system: $\mathbf{C}'_i = \{C_{ix'}, C_{iy'}, C_{iz'}\}$. Using (19) and (21), we can relate the equilibrium solution (6) to $\mathbf{X}$ by

$$N_i^{(\mathrm{eq})} = d(\mathbf{z}_0) + d'\mathbf{j}^{\mathrm{sol}} \cdot \mathbf{C}_i + \delta[\mathsf{K}^{(1)} \cdot \mathbf{X}] \cdot \mathbf{C}'_i + \tfrac{1}{2}\delta^2[\mathsf{K}^{(2)} \cdot \mathbf{X}] \cdot \mathbf{C}'_i \tag{25}$$

where the $[3 \times 8]$ matrices $\mathsf{K}^{(1)}$ and $\mathsf{K}^{(2)}$ relate respectively the first- and second-order derivatives coming into the Taylor approximation (21) of the momentum to the vector $\mathbf{X}$:

$$\mathsf{K}^{(1)} = \begin{pmatrix} 1 & 0 & 0 & 0 & 0 & 0 & 0 & 0 \\ 0 & 1 & 0 & 0 & 0 & 0 & 0 & 0 \\ 0 & 0 & 0 & 0 & 0 & 0 & 0 & 0 \end{pmatrix} \tag{26}$$

and

$$\mathsf{K}^{(2)} = \begin{pmatrix} 0 & 0 & 1 & 0 & 0 & 0 & 0 & 0 \\ 0 & 0 & 0 & 0 & 1 & 0 & 0 & 0 \\ 0 & 0 & 0 & -1 & 0 & -1 & 0 & 0 \end{pmatrix} \tag{27}$$

In order to relate the first-order correction $N_i^{(1)}$ to $\mathbf{X}$, all the derivatives appearing in (7) can be expressed in terms of the derivatives estimated on the wall at $\mathbf{z}_0^{\text{sol}}$, using the Taylor approximations (22). This formal procedure is simplified because the first-order term $N_i^{(1)}$ is invariant under any space isometry and has the same form in any orthogonal coordinate system. Thus $N_i^{(1)}$ becomes in the inclined coordinate system $\{x', y'; z'\}$

$$N_i^{(1)}(\mathbf{r}) = \frac{d'}{\lambda_\psi} \sum_{\alpha', \beta'} \frac{\partial j_{\alpha'}}{\partial \beta'}(\mathbf{r})\, Q_{i\alpha'\beta'} \tag{28}$$

where [cf. (11)]

$$Q_{i\alpha'\beta'} = C_{i\alpha'} C_{i\beta'} - \frac{c^2}{D} \delta_{\alpha'\beta'}, \qquad \{\alpha', \beta'\} \in \{x', y', z'\} \tag{29}$$

Using then the continuity equation (18), we can write $N_i^{(1)}(\mathbf{r})$ in the following vectorial form:

$$N_i^{(1)}(\mathbf{r}) = \frac{1}{\lambda_\psi} \mathbf{E}^{(1)}(\mathbf{r}) \cdot \mathbf{Q}_i' \tag{30}$$

where

$$\mathbf{E}^{(1)} = d'(E_{x'z'}, E_{x'x'}, E_{y'z'}, E_{y'y'}, E_{x'y'})(\mathbf{r}) \tag{31}$$

$$\mathbf{Q}_i' = (Q_{ix'z'}, Q_{ix'x'} - Q_{iz'z'}, Q_{iy'z'}, Q_{iy'y'} - Q_{iz'z'}, Q_{ix'y'}) \tag{32}$$

and the coefficients $E_{\alpha'\beta'}$ are given by

$$E_{\alpha'\beta'}(\mathbf{r}) = \left(\frac{\partial j_{\alpha'}}{\partial \beta'} + \frac{\partial j_{\beta'}}{\partial \alpha'}\right)(\mathbf{r}), \qquad \alpha' \neq \beta', \quad \{\alpha', \beta'\} \in \{x', y', z'\} \tag{33}$$

$$E_{\alpha'\alpha'}(\mathbf{r}) = \frac{\partial j_{\alpha'}}{\partial \alpha'}(\mathbf{r}), \qquad \alpha' \in \{x', y', z'\} \tag{34}$$

Applying the relations (22) and (23) to the coefficients (33) and (34) at the *boundary nodes*, we relate the first-order term $N_i^{(1)}(\mathbf{z}_0)$ to the vector $\mathbf{X}$ by

$$N_i^{(1)} = \frac{1}{\lambda_\psi} [\mathsf{G}^{(1)} \cdot \mathbf{X}] \cdot \mathbf{Q}_i' + \frac{\delta}{\lambda_\psi} [\mathsf{G}^{(2)} \cdot \mathbf{X}] \cdot \mathbf{Q}_i' \tag{35}$$

where the $[5 \times 8]$ matrices $G^{(1)}$ and $G^{(2)}$ are given by

$$G^{(1)} = \begin{pmatrix} 1 & 0 & 0 & 0 & 0 & 0 & 0 & 0 \\ 0 & 0 & 0 & 0 & 0 & 0 & 0 & 0 \\ 0 & 1 & 0 & 0 & 0 & 0 & 0 & 0 \\ 0 & 0 & 0 & 0 & 0 & 0 & 0 & 0 \\ 0 & 0 & 0 & 0 & 0 & 0 & 0 & 0 \end{pmatrix} \tag{36}$$

and

$$G^{(1)} = \begin{pmatrix} 0 & 0 & 1 & 0 & 0 & 0 & 0 & 0 \\ 0 & 0 & 0 & -1 & 0 & 0 & 0 & 0 \\ 0 & 0 & 0 & 0 & 1 & 0 & 0 & 0 \\ 0 & 0 & 0 & 0 & 0 & -1 & 0 & 0 \\ 0 & 0 & 0 & 0 & 0 & 0 & 1 & 1 \end{pmatrix} \tag{37}$$

By analogy with the first-order correction, the second-order term $N_i^{(2)}$ in (8) can be briefly written as

$$N_i^{(2)}(\mathbf{r}) = \frac{\nu}{\lambda_2} \mathbf{E}^{(2)}(\mathbf{r}) \cdot \mathbf{T}_i \tag{38}$$

the six-component vectors $\mathbf{E}^{(2)}(\mathbf{r})$ and $\mathbf{T}_i$ being

$$\mathbf{E}^{(2)}(\mathbf{r}) = d'(E_{xzz}, E_{zxx}, E_{yzz}, E_{zyy}, E_{yxx}, E_{xyy})(\mathbf{r}) \tag{39}$$

$$\mathbf{T}_i = (T_{ixzz}, T_{izxx}, T_{iyzz}, T_{izyy}, T_{iyxx}, T_{ixyy}) \tag{40}$$

The third-order eigenvectors $T_{i\alpha\beta\beta}$ are defined in (12); for FCHC model, the coefficients $E_{\alpha\beta\beta}$ are related to the second-order derivatives by [cf. (8)]

$$E_{\alpha\beta\beta}(\mathbf{r}) = \left[\frac{\partial^2 j_\alpha}{\partial \beta^2} + 2 \frac{\partial^2 j_\beta}{\partial \alpha \, \partial \beta} \right](\mathbf{r}), \qquad \{\alpha, \beta\} \in \{x, y, z\} \tag{41}$$

The term $N_i^{(2)}$ in (38) is not invariant by an arbitrary space isometry. Consequently, its form can change when the inclined coordinate system is used and we cannot simply replace $\{x, y, z\}$ with $\{x', y', z'\}$ in this term as done for the first-order term $N_i^{(1)}$ in (28). On the other hand, using (19) and (23), we can express the coefficients (41) in terms of the unknown second-order derivatives at the solid wall

$$\mathbf{E}^{(2)}(\mathbf{z}_0) = \frac{\nu}{\lambda_2} [\boldsymbol{\Xi} \cdot \mathbf{X}] \cdot \mathbf{T}_i \tag{42}$$

Here, the $[6 \times 8]$ matrix Ξ depends only upon the inclination of the solid wall; its two first columns, corresponding to the first-order derivatives in $\mathbf{X}$, are identically zero [cf. (27) and (37)]. In Section 3, the matrix Ξ is written for a solid wall parallel to a lattice axis.

Substituting relations (25), (35), and (42) into the Chapman–Enskog expansion (5), the second-order approximation of the populations at the boundary nodes

$$N_i(\mathbf{z}_0) = d(\mathbf{z}_0) + d'\mathbf{j}^{\text{sol}} \cdot \mathbf{C}_i + \mathbf{X}(\mathbf{z}_0) \cdot \mathbf{e}_i(\mathbf{z}_0) \tag{43}$$

where the vector $\mathbf{e}_i(\mathbf{z}_0)$ is given by

$$\begin{aligned} \mathbf{e}_i = {} & \delta \mathsf{K}^{(1)t} \cdot \mathbf{C}'_i + \frac{1}{2}\delta^2 \mathsf{K}^{(2)t} \cdot \mathbf{C}'_i \\ & + \frac{1}{\lambda_\psi} \mathsf{G}^{(1)t} \cdot \mathbf{Q}'_i + \frac{\delta}{\lambda_\psi} \mathsf{G}^{(2)t} \cdot \mathbf{Q}'_i \\ & + \frac{\nu}{\lambda_2} \Xi^t \cdot \mathbf{T}_i, \qquad i \in \{1, \ldots, b_m\} \end{aligned} \tag{44}$$

The superscript t denotes the transpose operator. Thus, eight components of the vector $\mathbf{X}(\mathbf{z}_0)$ are to be found at each boundary node in order to construct the population solution. It is important to repeat here that local density $d(\mathbf{z}_0)$ is also considered to be unknown.

The populations $N_i^{\text{out}}(\mathbf{z}_0, t)$ leaving the lattice after collision at time $t-1$ can be derived from (43) with the help of the lattice Boltzmann equation (1):

$$\begin{aligned} N_i^{\text{out}}(\mathbf{z}_0, t) = {} & d(\mathbf{z}_0, t-1) + d'\mathbf{j}^{\text{sol}} \cdot \mathbf{C}_i \\ & + \mathbf{X}(\mathbf{z}_0, t-1) \cdot \mathbf{e}_i^{\text{out}} + d'\rho(\mathbf{z}_0, t-1)\, \mathbf{F} \cdot \mathbf{C}_i, \qquad i \in \{1, \ldots, b_m\} \end{aligned} \tag{45}$$

with

$$\mathbf{e}_i^{\text{out}} = \sum_{j=1}^{b_{ni}} \mathscr{A}_{ij} \cdot \mathbf{e}_j \qquad i \in \{1, \ldots, b_m\} \tag{46}$$

Since the vectors $\mathbf{C}_{\alpha'}$, $\mathbf{Q}_{\alpha'\beta'}$, and $\mathbf{T}_{\alpha\beta\beta}$ are the eigenvectors of the collision matrix, the derivation of $\mathbf{e}_i^{\text{out}}$ is straightforward. For stationary solutions, we can replace $d(\mathbf{z}_0, t-1)$ by $d(\mathbf{z}_0, t)$ and $\mathbf{X}(\mathbf{z}_0, t-1)$ by $\mathbf{X}(\mathbf{z}_0, t)$ in the right-hand side of (45). However, the forcing term in (45) is actually calculated at time $t-1$ [see (1)] and is hence known.

2.5. Second-Order Solution for the Unknown Populations

2.5.1. Linear Equations for the Unknown Coefficients. We must now compute $\mathbf{X}(\mathbf{z}_0, t)$ from (43)–(46). This step requires an appropriate subset of known populations from the sets $\{N_i^{\text{loc}}(\mathbf{z}_0, t)\}$ and (or) $\{I_i^{\text{out}}(\mathbf{z}_0, t)\}$. Let $I^{\text{use}}(\mathbf{z}_0)$ be a new set of indices for these chosen populations. Each, $j \in I^{\text{use}}(\mathbf{z}_0)$ has a corresponding index i either in $I^{\text{loc}}(\mathbf{z}_0)$ or in $I^{\text{out}}(\mathbf{z}_0)$. Let us denote $N^{\text{use}}(\mathbf{z}_0, t)$ the corresponding known contribution to (43) or (45) and $\mathbf{e}_j^{\text{use}}$ the corresponding vector $\mathbf{e}_i$ or $\mathbf{e}_i^{\text{out}}$. In the first case,

$$N_j^{\text{use}}(\mathbf{z}_0, t) = N_i^{\text{loc}}(\mathbf{z}_0, t) - d'\mathbf{j}^{\text{sol}} \cdot \mathbf{C}_i \tag{47}$$

and in the second one

$$N_j^{\text{use}}(\mathbf{z}_0, t) = N_i^{\text{out}}(\mathbf{z}_0, t) - \{d'\mathbf{j}^{\text{sol}} \cdot \mathbf{C}_i + d'\rho(\mathbf{z}_0, t-1)\,\mathbf{F} \cdot \mathbf{C}_i\} \tag{48}$$

Using these notations, we can express Eqs. (43) and (45) in the same way:

$$\mathbf{e}_j^{\text{use}}(\mathbf{z}_0) \cdot \mathbf{X}(\mathbf{z}_0) = N_j^{\text{use}}(\mathbf{z}_0) - d(\mathbf{z}_0), \qquad j \in I^{\text{use}}(\mathbf{z}_0) \tag{49}$$

It follows that a vector $\mathbf{X}$ can be obtained from (49) for any subset of eight populations N_j^{use} such that the corresponding $[8 \times 8]$ matrix $\mathbf{e}^{\text{use}}$ is invertible. In Section 3, we show that there exists at least one subset when the wall is parallel to the y axis. In general several subsets giving an invertible matrix $\mathbf{e}^{\text{use}}$ can be found, i.e., there exists a family of LSOB closure relations. The study of this family and the existence of a possible "best" choice among its elements is left for future work. Of course all the acceptable LSOB closure relations yield the same N_i^{in} populations for flows such that the $O(\varepsilon^3)$ terms vanish in the Chapman–Enskog expansion. For general flows, a third-order difference is expected between the N_i^{in} populations derived from different subsets.

For general Dirichlet conditions (nonuniform momentum), some derivatives appearing in (17) are nonzero (but known) and the unknown derivatives are those entering the vector $\mathbf{X}$ defined in (20). Then the linear system (49) is unchanged, but the contributions of the known nonzero derivatives to the second-order Chapman–Enskog expansion must be included in (47) and (48), as done for the nonzero momentum $\mathbf{j}^{\text{sol}}$.

Since the linear system (49) is local, each boundary node can be considered independently. The method becomes especially transparent for the rather artificial case of a known density distribution. Thus, let us consider this case first.

2.5.2. LSOB Method for Flows with a Known Density (Artificial Case). When the density in (49) is known and provided that $\det[\mathbf{e}^{use}]$ is different from zero, the solution for $\mathbf{X}$ can be immediately derived from (49). Substitution of this solution in (43) gives the unknown populations N_i^{in} in the following form [cf. (15)]:

$$N_i^{in}(\mathbf{z}_0) = d\left\{1 - \sum_{j \in I^{use}} P_{ij}\right\} + d'\mathbf{j}^{sol} \cdot \mathbf{C}_i + \sum_{j \in I^{use}} P_{ij} N_j^{use}, \qquad i \in I^{in}(\mathbf{z}_0) \quad (50)$$

where the elements of the matrix $\mathbf{P}(\mathbf{z}_0)$ are simply

$$P_{ij} = \mathbf{e}_i \cdot [\mathbf{e}^{use}]_j^{-1}, \qquad i \in I^{in}(\mathbf{z}_0), \quad j \in I^{use}(\mathbf{z}_0) \quad (51)$$

Here $[\mathbf{e}^{use}]_j^{-1}$ denotes the jth column of the matrix $[\mathbf{e}^{use}]^{-1}$. Note that the solution (50) becomes density independent if and only if $\mathbf{P}$ is a transition matrix

$$\sum_{j \in I^{use}} P_{ij} = 1 \quad (52)$$

Note also that the classical reflections—bounceback, specular, or a local combination of the two—represent very particular cases of (50) when (52) is *explicitly* introduced.

2.5.3. LSOB Method for Flows with Unknown Density (General Case). Let us now replace the unknown density in (43), (45) and in the linear system (49) by its definition [see (2) and (9)]

$$d = b_m^{-1} \left\{ \sum_{i \in I^{loc}(\mathbf{z}_0)} N_i^{loc} + \sum_{i \in I^{in}(\mathbf{z}_0)} N_i^{in} \right\} \quad (53)$$

The substitution of (50) with (53) in the sum of relations (43) for populations $N_i^{in}[i \in I^{in}(\mathbf{z}_0)]$ gives the *solution for local density* with a third-order error $O(\varepsilon^3)$:

$$d = \frac{1}{\mathscr{D}_\Sigma} \left\{ \sum_{i \in I^{loc}(\mathbf{z}_0)} N_i^{loc} + d'\mathbf{j}^{sol} \cdot \sum_{i \in I^{in}(\mathbf{z}_0)} \mathbf{C}_i + \sum_{i \in I^{in}(\mathbf{z}_0)} \sum_{j \in I^{use}(\mathbf{z}_0)} P_{ij} \cdot N_j^{use} \right\} \quad (54)$$

$$\mathscr{D}_\Sigma = L^{loc} + \sum_{j \in I^{use}(\mathbf{z}_0)} \sum_{i \in I^{in}(\mathbf{z}_0)} P_{ij}$$

where L^{loc} is the *total* number of populations N_i^{loc} at the node $\mathbf{z}_0$ as defined in section 2.2. Thus, the local density is automatically obtained as a linear combination of the populations N_i^{loc} and N_j^{use} provided that $\mathscr{D}_\Sigma$ is nonzero.

When (54) is substituted in (50), the solution for the unknown populations becomes the following linear combination of the populations N_i^{loc}, and N_j^{use}:

$$N_i^{\text{in}} = d'\mathbf{j}^{\text{sol}} \cdot \left\{ \mathbf{C}_i + P_i^{\text{loc}} \sum_{i \in I^{\text{in}}(\mathbf{z}_0)} \mathbf{C}_i \right\} + P_i^{\text{loc}} \sum_{j \in I^{\text{loc}}} N_j^{\text{loc}} + \sum_{j \in I^{\text{use}}} P_{ij}^{\text{use}} N_j^{\text{use}}, \qquad i \in I^{\text{in}}(\mathbf{z}_0) \tag{55}$$

where

$$P_i^{\text{loc}} = \frac{1}{\mathscr{D}_\Sigma} \left\{ 1 - \sum_{j \in I^{\text{use}}} P_{ij} \right\}, \qquad i \in I^{\text{in}}(\mathbf{z}_0) \tag{56}$$

the elements of the matrix $\mathbf{P}^{\text{use}}$ are

$$P_{ij}^{\text{use}} = P_{ij} + P_i^{\text{loc}} \sum_{k \in I^{\text{in}}(\mathbf{z}_0)} P_{kj}, \qquad i \in I^{\text{in}}(\mathbf{z}_0), \qquad j \in I^{\text{use}}(\mathbf{z}_0) \tag{57}$$

and the matrix $\mathbf{P}$ is introduced in (51).

The principal result of the relations (55)–(57) is that the unknown populations are determined correctly, with a third-order error $O(\varepsilon^3)$, as a linear combination of the known populations supplied by the lattice Boltzmann equation (1). The coefficients of this combination are functions of the inclination of the solid wall, its velocity, the distance between the wall and the boundary node, and the eigenvalues of the collision matrix [see (44)]. They depend also upon the local distribution of known and unknown populations through the term $\mathscr{D}_\Sigma$ [see (54)]. From considerations of linear stability in some simplified geometry (see Appendix B), the lattice Boltzmann equation (1) with the boundary conditions (55)–(57) is expected to be stable at least when the solid wall is located *outside* the lattice ($\delta \leqslant 0$).

For each boundary node $\mathbf{z}_0$, we can summarize the LSOB method as follows. The distance to the assumed solid wall is computed and the vectors $\mathbf{e}_i(\mathbf{z}_0)$ are constructed for all the populations at the boundary node $\mathbf{z}_0$, using the desired inclination of the solid wall and the chosen eigenvalues λ_ψ and λ_2 [cf. (44)]. Then a subset of populations $\{N_j^{\text{use}}(\mathbf{z}_0), j \in I^{\text{use}}(\mathbf{z}_0)\}$ is chosen and the matrix of boundary conditions $\mathbf{P}^{\text{use}}(\mathbf{z}_0)$ is computed from the corresponding matrix $\mathbf{e}^{\text{use}}(\mathbf{z}_0)$ [cf. (51), (54), and (57)]. All these steps are done only once for each boundary node during the initialization procedure. Then the unknown populations are computed from the relations (55)–(57) for each time step of the iteration procedure.

2.6. Conservation of Mass

It is noteworthy that there is no reason for the sum of the unknown populations computed with the LSOB method to be equal to the sum of the populations leaving the lattice. Thus, in general, one should expect to detect some change in the total mass $\Delta M(t)$,

$$\Delta M(t) = \sum_{\mathbf{z}_0} \sum_{i \in I^{\text{out}}(\mathbf{z}_0)} N_i^{\text{out}}(\mathbf{z}_0, t) - \sum_{\mathbf{z}_0} \sum_{i \in I^{\text{in}}(\mathbf{z}_0)} N_i^{\text{in}}(\mathbf{z}_0, t) \tag{58}$$

i.e., a nonzero mass flux across the boundaries.

This possibility that the total mass is not conserved in general flows represents the principal difference between explicit methods and classical reflections. Although it is tantalizing to enforce the mass conservation in the LSOB method using locally the additional constraint $\Delta M(t) = 0$ at each time step t, we show in the next section that local conservation of mass leads to non hydrodynamic boundary layers for Couette and Poiseuille flows in inclined channels.

Since the local mass is exactly conserved by the collision operator, the total mass in any bounded domain is also exactly conserved for any steady flow. It follows that $\Delta M \equiv 0$ for any steady flow if the summations in (58) are taken for all the boundary nodes of the computational domain. However even if the lack of mass disappears for steady flows, it can exist when the stationary regime is not yet reached. In addition, the global conservation of mass does not imply that the total mass flux across any side of the domain should be exactly zero. For particular flows, exactly given by the second-order Chapman–Enskog expansion and having a zero mass flux across some sides of the computational domain, the LSOB method gives a zero mass flux across these sides. This is the case for the two walls parallel to Couette and Poiseuille flows, as shown analytically in Appendix A. For more general steady flows, the best which can be expected from LSOB method is $\Delta M = O(\varepsilon^3)$, since the terms $O(\varepsilon^3)$ have been neglected.

Let us first compute ΔM for a general steady flow near a solid boundary parallel to the xy plane of the FCHC lattice, without forcing terms ($F_z = 0$). Substituting in (58) the second-order approximations of N_i^{in} and N_i^{out} given by (43)–(46) yields the following mass flux across the boundary:

$$\Delta M = 12 d' \sum_{\mathbf{z}_0^{\text{sol}}} \left\{ j_z^{\text{sol}} - \frac{\delta}{2} \left(\delta + \frac{2}{3} \right) \frac{\partial^2 j_z^{\text{sol}}}{\partial z^2} \right\} \tag{59}$$

Hence, when the normal velocity is zero at the wall ($j_z^{\text{sol}} = 0$), the mass flux is proportional to $\partial^2 j_z^{\text{sol}} / \partial z^2$. Except for the particular wall locations $\delta = -2/3$ and $\delta = 0$ (wall located on the boundary lattice nodes), the mass

flux is of order $O(\varepsilon^2)$ when the derivative $\partial^2 j_z^{sol}/\partial z^2$ is $O(1)$, e.g., stagnation flow near an *infinite* solid plane.[25] A similar calculation for a solid wall parallel to the y axis and inclined at 45° with the x axis (still parallel to some of the FCHC velocities) shows a dependence of ΔM with $\partial^2 j_{z'}^{sol}/\partial z'^2$ which does not vanish for $\Delta = 0$ and $\delta = -2/3$, but for other values of the minimum distance between the lattice nodes and the wall. Preliminary calculations for more general orientations of the wall have shown a similar dependence of the mass flux with the second-order derivatives of the momentum. Unfortunately the coefficients depend upon the details of the discretization of the boundary and we do not even know if they can vanish for some values of the minimum distance between the lattice nodes and the wall, as observed for the previous orientations.

From these results, it appears that the user is faced with two choices: to keep the third-order precision of the LSOB method at the possible expense of a second-order mass flux across some sides of the boundary, or to prescribe a zero mass flux across each side of the boundary (for instance, by a nonlocal distribution of ΔM between the unknown populations at the boundary nodes) at the expense of a second-order precision when $\partial^2 j_{z'}^{sol}/\partial z'^2$ is $O(1)$. The actual choice will probably depend on the properties of the simulated flow.

3. FLAT SOLID WALL PARALLEL TO THE y AXIS

3.1. 3D Flow

In the previous sections we have not made any assumption about the inclination of the solid boundary with the lattice axes. However, in order to demonstrate the method in some detail and, in particular, in order to determine the subsets of the populations N_j^{use}, one must find all the possible local neighborhood of the boundary nodes appearing from the discretization of an inclined flat wall on the FCHC lattice. This rather complicated problem becomes much simpler if the solid wall is assumed to be parallel to one axis, say y, but arbitrarily inclined with the two other ones, x and z. This simplified geometry still remains quite general compared to the solid walls parallel to a lattice plane that are usually considered.

Let θ be the angle of the wall with the x axis; the associated orthogonal coordinate system is

$$\begin{aligned} x' &= x\cos\theta + z\sin\theta \\ z' &= -x\sin\theta + z\cos\theta \\ y' &= y \end{aligned} \tag{60}$$

and the $[6\times 8]$ matrix Ξ in (42) is given by relations

$$
\begin{aligned}
E_{xzz} &= \cos\theta\,(\cos^2\theta - 2\sin^2\theta)\,\frac{\partial^2 j_{x'}}{\partial z'^2} \\
&\quad + \sin\theta\,(7\cos^2\theta - 2\sin^2\theta)\,\frac{\partial^2 j_{x'}}{\partial x'\,\partial z'} + 3\sin\theta\cos^2\theta\,\frac{\partial^2 j_{y'}}{\partial y'\,\partial z'} \\
E_{zxx} &= \sin\theta\,(\sin^2\theta - 2\cos^2\theta)\,\frac{\partial^2 j_{x'}}{\partial z'^2} \\
&\quad + \cos\theta\,(2\cos^2\theta - 7\sin^2\theta)\,\frac{\partial^2 j_{x'}}{\partial x'\,\partial z'} - 3\sin^2\theta\cos\theta\,\frac{\partial^2 j_{y'}}{\partial y'\,\partial z'} \\
E_{yzz} &= \cos^2\theta\,\frac{\partial^2 j_{u'}}{\partial z'^2} + \sin 2\theta\left\{\frac{\partial^2 j_{x'}}{\partial y'\,\partial z'} + \frac{\partial^2 j_{y'}}{\partial x'\,\partial z'}\right\} \\
E_{zyy} &= 2\cos\theta\,\frac{\partial^2 j_{y'}}{\partial y'\,\partial z'} \\
E_{yxx} &= \sin^2\theta\,\frac{\partial^2 j_{y'}}{\partial z'^2} - \sin 2\theta\left\{\frac{\partial^2 j_{x'}}{\partial y'\,\partial z'} + \frac{\partial^2 j_{y'}}{\partial x'\,\partial z'}\right\} \\
E_{xyy} &= -2\sin\theta\,\frac{\partial^2 j_{y'}}{\partial y'\,\partial z'}
\end{aligned}
\tag{61}
$$

Analyzing the relations (27), (37), and (61), one sees that the derivatives $\partial^2 j_{x'}/\partial y'\,\partial z'$ and $\partial^2 j_{y'}/\partial x'\,\partial z'$ come into (43) with equal coefficients e_{i7} and e_{i8} for walls parallel to the y axis:

$$
e_{i7} = \frac{\delta}{\lambda_\psi}\,Q_{ix'y'} + \frac{\nu}{\lambda_2}\sin 2\theta\,(T_{iyzz} - T_{iyxx}), \qquad e_{i8} = e_{i7}, \qquad i \in \{1,\ldots, b_m\} \tag{62}
$$

Hence, in order to obtain $\det[\mathbf{e}^{\text{use}}] \neq 0$, the second-order approximation (43) must be written

$$
N_i(\mathbf{z}_0) = d(\mathbf{z}_0) + d'\mathbf{j}^{\text{sol}} \cdot \mathbf{C}_i + \mathbf{X}^{\|}(\mathbf{z}_0) \cdot \mathbf{e}_i^{\|}(\mathbf{z}_0) \tag{63}
$$

where the seventh component of $\mathbf{X}^{\|}(\mathbf{z}_0)$ is the sum of the last two components of the vector $\mathbf{X}(\mathbf{z}_0)$

$$
\mathbf{X}^{\|}(\mathbf{z}_0) = d'\left(\frac{\partial j_{x'}}{\partial z'}, \frac{\partial j_{y'}}{\partial z'}, \frac{\partial^2 j_{x'}}{\partial z'^2}, \frac{\partial^2 j_{x'}}{\partial x'\,\partial z'}, \frac{\partial^2 j_{y'}}{\partial z'^2}, \frac{\partial^2 j_{y'}}{\partial y'\,\partial z'}, \frac{\partial^2 j_{x'}}{\partial y'\,\partial z'} + \frac{\partial^2 j_{y'}}{\partial x'\,\partial z'}\right)(\mathbf{z}_0^{\text{sol}}) \tag{64}
$$

and the seven components of the vector $\mathbf{e}_i^{\parallel}$ are the first seven components of the vector $\mathbf{e}_i$ defined in (44). Note that for a solid wall parallel to the (x, y) lattice plane ($\theta = 0°$) and located exactly on the last lattice nodes ($\delta = 0$), the last component $\mathbf{e}_{i7}^{\parallel}$ of $\mathbf{e}_i^{\parallel}$ becomes equal to zero [cf. (62)]. In order to avoid $\det[\mathbf{e}^{\text{use}}] = 0$, only the first six components of $\mathbf{X}_i^{\parallel}$ and $\mathbf{e}_i^{\parallel}$ must be used in (63) for the particular case $\theta = 0°$, $\delta = 0$.

3.2. 2D Flows

The users of lattice Boltzmann methods often consider 2D flows. When the flow is parallel to some lattice plane, say (x, z), it can be simulated on the FCHC lattice with periodical boundary conditions in the y direction. In such a case, the second-order solution for 2D flows will be automatically obtained when the LSOB method is applied in its general 3D form. However, since the y component of the momentum and the momentum derivatives along the y axis are equal to zero for such flows, the second-order approximation of the populations can be written in the following reduced 2D form:

$$\begin{aligned} N_i(\mathbf{z}_0) &= d(\mathbf{z}_0) + d'\mathbf{j}^{\text{sol}} \cdot \mathbf{C}_i + \mathbf{X}^{\text{2D}}(\mathbf{z}_0) \cdot \mathbf{e}_i^{\text{2D}}(\mathbf{z}_0) \\ \mathbf{j} &= \{ j_{x'}(x', z'), j_{z'}(x', z') \} \end{aligned} \tag{65}$$

where

$$\mathbf{X}^{\text{2D}}(\mathbf{z}_0) = d' \left(\frac{\partial j_{x'}}{\partial z'}, \frac{\partial^2 j_{x'}}{\partial z'^2}, \frac{\partial^2 j_{x'}}{\partial x' \, \partial z'} \right) (\mathbf{z}_0^{\text{sol}}) \tag{66}$$

and the three components of the vector $\mathbf{e}_i^{\text{2D}}$ are, accordingly, the first, third, and fourth components of the vector $\mathbf{e}_i$ defined in (44). Thus, the LSOB method needs only three populations N_j^{use} to determine boundary conditions with third order error for two dimensional flows.

3.3. Some Particular Sets of Known Populations

In order to apply the LSOB method on any boundary node $\mathbf{z}_0$ one must choose the populations $N_j^{\text{use}}(\mathbf{z}_0)$ [see (47)–(49)] in such a way that the corresponding matrix $\mathbf{e}^{\text{use}}$ is invertible and the value of $\mathscr{D}_{\Sigma}$ in (54) is nonzero for the inclination θ of the given solid wall, the distance δ between $\mathbf{z}_0$ and the wall, and the chosen eigenvalues of the collision matrix.

At this point it becomes necessary to label explicitly the 18 different velocities of the 3D FCHC model; let us use the following choice:

$$
\begin{aligned}
&\mathbf{C}_1=(1,0,0), && \mathbf{C}_2=(1,0,1), && \mathbf{C}_3=(0,0,1)\\
&\mathbf{C}_4=(-1,0,1), && \mathbf{C}_5=(-1,0,0), && \mathbf{C}_6=(0,1,1)\\
&\mathbf{C}_7=(0,-1,1), && \mathbf{C}_8=(0,1,0), && \mathbf{C}_9=(0,-1,0)\\
&\mathbf{C}_{10}=(1,1,0), && \mathbf{C}_{11}=(-1,1,0), && \mathbf{C}_{12}=(-1,-1,0)\\
&\mathbf{C}_{13}=(1,-1,0), && \mathbf{C}_{14}=(0,0,-1), && \mathbf{C}_{15}=(-1,0,-1)\\
&\mathbf{C}_{16}=(0,1,-1), && \mathbf{C}_{17}=(0,-1,-1), && \mathbf{C}_{18}=(1,0,-1)
\end{aligned}
\tag{7}
$$

When the solid wall is parallel to the y axis and $0° \leqslant \theta \leqslant 45°$, five kinds of boundary nodes, denoted r_1 to r_5 in Figs. 2a and 2b, can appear for the natural "stair-type" discretization on the FCHC lattice, defined such that the algebraic distance δ from these nodes to the wall is negative and

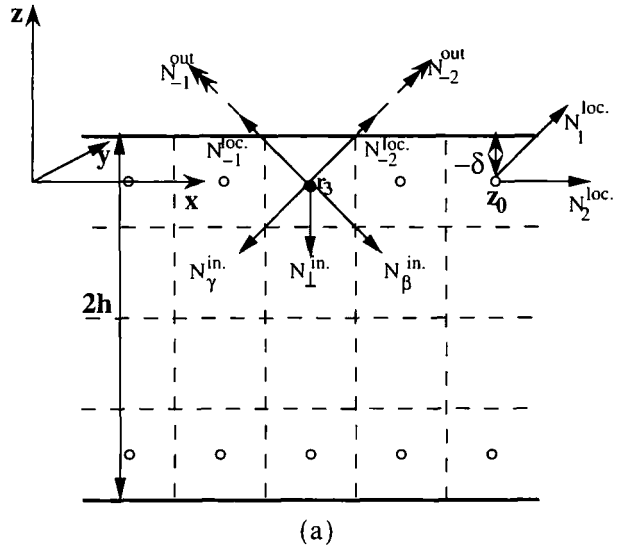

Fig. 2. Two-dimensional section of noninclined and inclined channels parallel to the y axis: (a) $\theta = 0°$; (b) $\tan\theta = 3/5$.

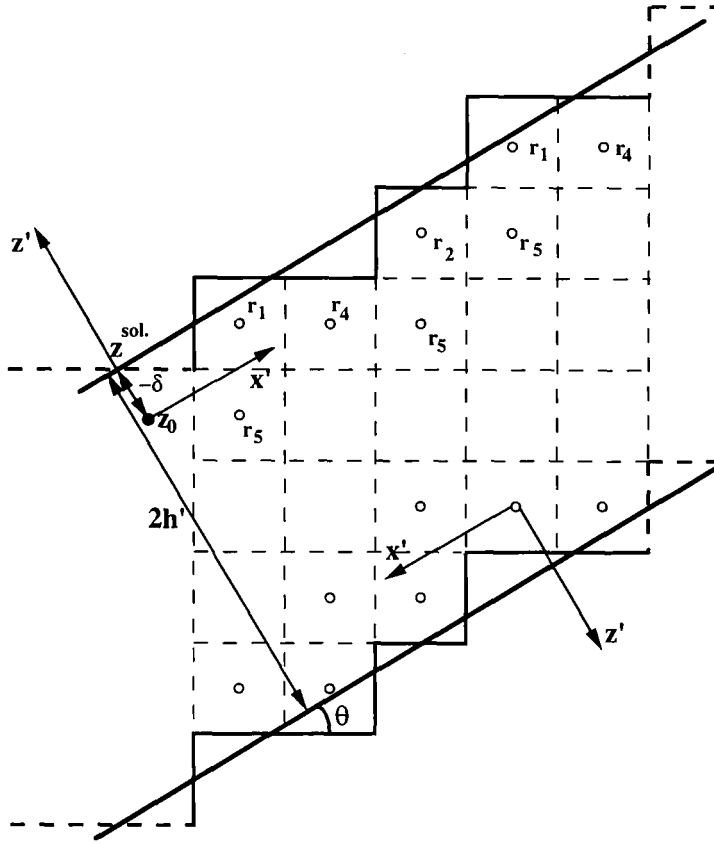

(b)

Fig. 2 *(Continued)*

there are at most two consecutive boundary nodes in the direction. These nodes r_1 to r_5 can be described as follows:

$$\begin{aligned}
&\text{node } r_1\text{: } L^+ = 10, \quad L^- = 8, \quad I^{\text{loc}} = \{2,..., 9, 11, 12\} \\
&\text{node } r_2\text{: } L^+ = 11, \quad L^- = 7, \quad I^{\text{loc}} = \{2,..., 9, 11, 12, 15\} \\
&\text{node } r_3\text{: } L^+ = 13, \quad L^- = 5, \quad I^{\text{loc}} = \{1,..., 13\} \\
&\text{node } r_4\text{: } L^+ = 14, \quad L^- = 4, \quad I^{\text{loc}} = \{1,..., 13, 15\} \\
&\text{node } r_5\text{: } L^+ = 17, \quad L^- = 1, \quad I^{\text{loc}} = \{1,..., 17\}
\end{aligned} \tag{68}$$

where L^+ (L^-) is the number of known (resp. unknown) populations in the node $\mathbf{z}_0$ ($L^+ + L^- = 18$ for the 3D projection of the FCHC lattice; in this case the populations 1, 3, 5, 8, and 14 must be counted twice). Note that for $\theta = 0°$ all the boundary nodes are of the r_3 type (see Fig. 2a) and the pattern $\{r_2, r_5\}$ repeats itself for $\theta = 45°$. When θ is not in the range $[0°, 45°]$, the description of the other possible boundary nodes is derived from (68) through the symmetry group of the FCHC lattice.

Obviously, it is much simpler to have the same subset of the populations N_j^{use} for any local geometry appearing from the discretization of a given wall. For a solid wall parallel to a lattice axis and for the "stair-type" discretization, we have verified that such subsets can be extracted from the populations N_i^{loc}, i.e., without using the populations N_i^{out}. Except for some particular combinations of the eigenvalues λ_ψ, λ_2 and the parameter δ, these solutions give $\det[\mathbf{e}^{\text{use}}] \neq 0$ in (49) and $\mathscr{D}_\Sigma \neq 0$ in (54) when the wall is located *outside* the lattice and the eigenvalues of the collision matrix satisfy the linear stability conditions[2] i.e., they are taken in the interval $]-2, 0[$.

Simulating 2D flows, one can take the following subset of known populations N_i^{loc} for any local geometry r_1 to r_5 [cf. (66)]

$$I^{\text{use}} = \{2, 3, 4\} \tag{69}$$

When the flow is 3D, one can take, for instance, in ordinary nodes r_3 for a noninclined wall ($\theta = 0°$) or in any node r_1–r_5 appearing from the discretization of the inclined wall the following subsets of the known populations N_i^{loc}:

$$\begin{aligned} I^{\text{use}} &= \{3, 4, 5, 6, 7, 11, 13\}, \qquad \theta = 0°, \quad \delta \neq 0 \\ I^{\text{use}} &= \{3, 4, 5, 6, 7, 11\}, \qquad \theta = 0°, \quad \delta = 0 \\ I^{\text{use}} &= \{2, 3, 4, 6, 7, 8, 11\}, \qquad 0° < \theta \leqslant 45° \end{aligned} \tag{70}$$

It should be mentioned that the subsets I^{use} in (69) and (70) are not the only solutions; one can find other subsets of the known populations N_i^{loc} or N_i^{out} or even use linear combinations of these populations.

However, the generalization of these boundary conditions to more complicated walls, such as walls with a more general inclination or smooth surfaces, will require characterizing all the possible types of boundary nodes and finding a systematic algorithm to choose the populations N_j^{use} at these nodes. These tasks remain to be done.

3.4. Application of LSOB Method to Poiseuille and Couette Flows

Poiseuille and Couette flows parallel to some principal lattice link represent the usual test solutions. For Poiseuille flows parallel to a population velocity, the only problem of lattice Boltzmann simulations with classical reflections is the effective location of no-slip walls with respect to the computational domain.[15-20] When the bounceback condition is used, it is shown in ref. 16 that the effective width of the channel parallel to some lattice link depends upon its inclination and some function of the eigenvalues λ_ψ and λ_2 (see ref. 24 for further discussions about this function).

3.4.1. Poiseuille Flows in Inclined Channels. Two kinds of stationary Poiseuille flows can be considered in a channel with solid walls parallel to the y axis ($y' = y$) and arbitrarily inclined with respect to the x axis. In the first case, the flow is parallel to the x' axis [see (60)]; in the second case the flow is parallel to the y axis. Both flows depend only on the coordinate z' and the forcing term can be described in a uniform manner

$$-\rho F_{\alpha'} = \nu \frac{\partial^2 j_{\alpha'}}{\partial z'^2}, \qquad -h' \leqslant z' \leqslant h', \quad \alpha' = x' \quad \text{or} \quad \alpha' = y, \quad \rho = \rho_0 \tag{71}$$

For such flows, the second-order Chapman–Enskog expansion gives the exact solution since higher order derivatives vanish,

$$N_i(\mathbf{r}) = d + d' j_{\alpha'}(\mathbf{r})\, C_{i\alpha'} + \frac{d' \partial j_{\alpha'}}{\lambda_\psi\, \partial z'}(\mathbf{r})\, Q_{i\alpha' z'} + \frac{\nu}{\lambda_2} \mathbf{E}^{(2)}(\mathbf{r}) \cdot \mathbf{T}_i \tag{72}$$

The term $\mathbf{E}^{(2)}(\mathbf{r}) \cdot \mathbf{T}_i$ is written in (38)–(41). When the external force (1) is applied to simulate constant pressure gradient, the density d is constant (see discussion in ref. 24 for more details). Moreover, the second-order term $\mathbf{E}^{(2)}(\mathbf{r}) \cdot \mathbf{T}_i$ is invariant by the rotation for Poiseuille flows (see Appendix A).

Figure 3 shows the profiles across the channel of the normalized differences between the numerical and expected solutions for the density and the normal and tangential momenta obtained with LSOB and bounceback conditions. For all the profiles the normalization factor is $h'/j^{\max}$, $j^{\max}$ being the theoretical peak momentum in the Poiseuille flow and h' the expected half-width of the channel: $h' = h \cos\theta$ and $\tan\theta = 3/5$.

As shown by the zero-value lines in Fig. 3, the LSOB method provides an exact analytical solution for any inclination and for any channel width.

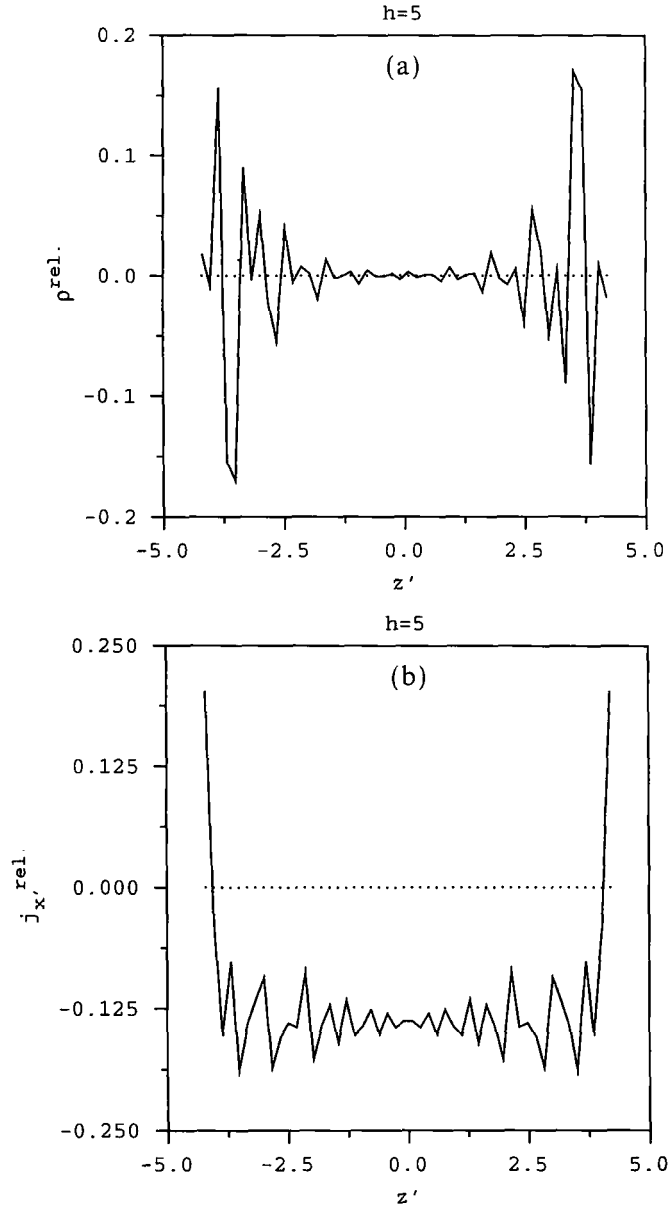

Fig. 3. Profiles of the normalized difference between numerical and theoretical solution for two Poiseuille flows: (a, d) density ρ, (b, e) tangential momentum $j_{x'}$ and, (c, f) normal momentum $j_{z'}$. The normalization factor is $h'/j^{\max}$, $j^{\max}$ being the theoretical peak momentum in the Poiseuille flow and h' the expected half-width of the channel; $h' = h \cos\theta$ and $\tan\theta = 3/5$. The solid lines are obtained for bounceback condition and the dotted zero-value ones for the LSOB method. The simulations are performed with the same viscosity and body force; all the eigenvalues of the collision matrix are equal to -1. The results are shown for two sizes of the computational domain: $h = 5$ (a–c) and $h = 20$ (d–f).

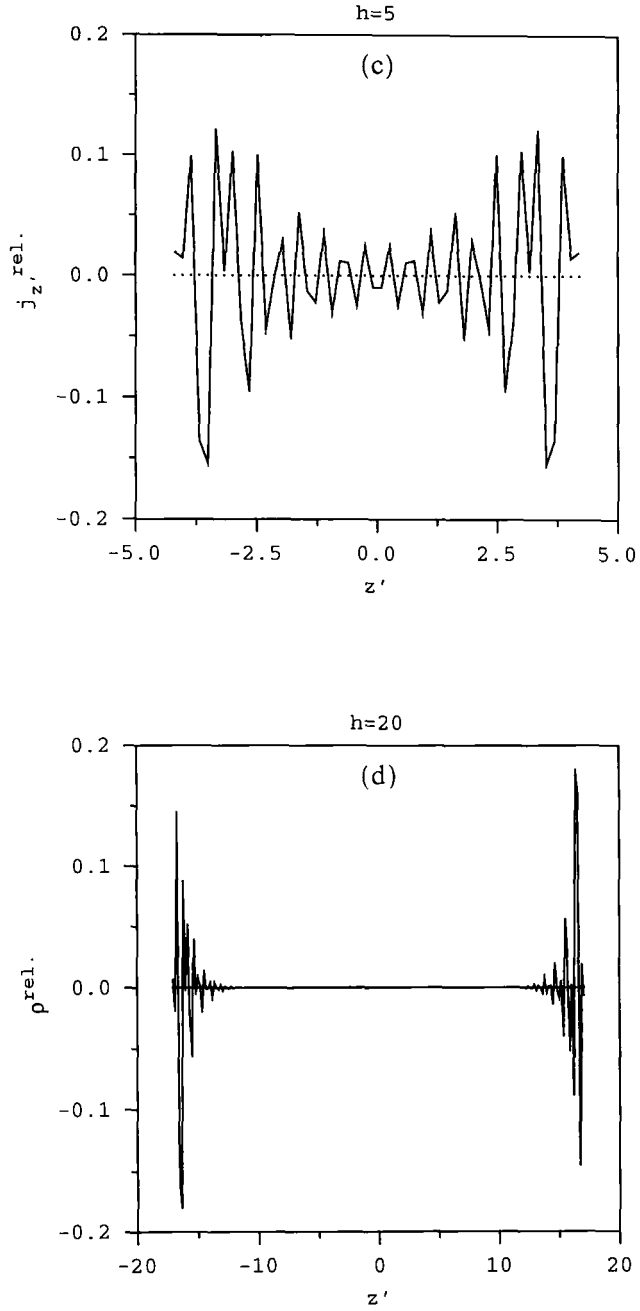

Fig. 3 *(Continued)*

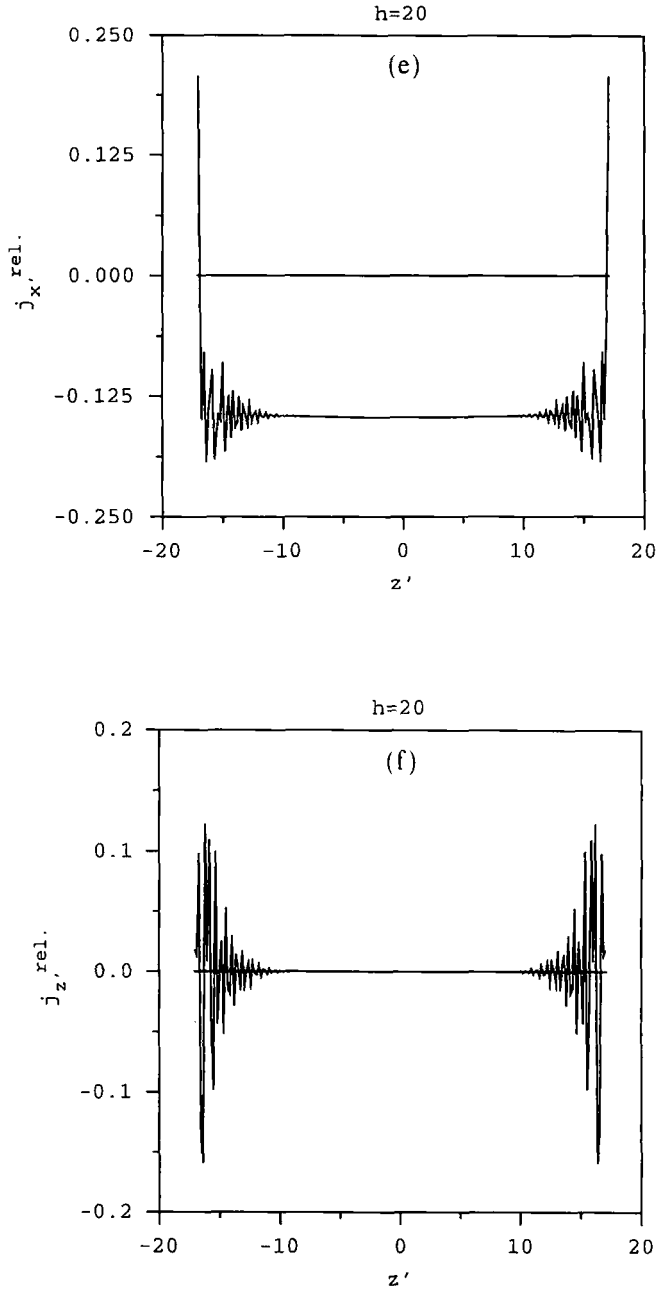

Fig. 3 *(Continued)*

This is due to the fact that for such flows the second-order expansion (72) represents the exact solution and the total mass is automatically conserved by the LSOB method (as shown in Appendix A for the simplified discretization given in Fig. 4). The width of the channel is fixed by the choice of the computational domain and the distance δ; the inclination is controlled by the construction of the LSOB conditions at each boundary node [cf. (43)–(44)]. All the different implementations of LSOB method simulate exactly the Poiseuilie solutions: the density can be assumed either known or unknown, and the method can use either the general 3D solution (43)–(44) or its 2D form (65), or even the shorter 1D form given in Appendix A; the possible subsets of the known populations N_j^{use} for the upper wall can be taken either in (69) or in (70) (the populations for the lower wall being found by symmetry).

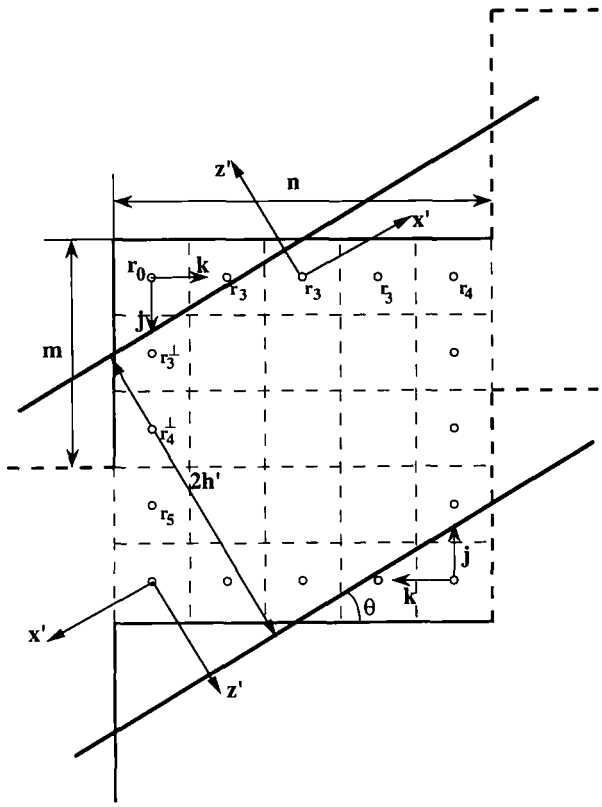

Fig. 4. "Rough" discretization of a solid wall parallel to the y axis for $\tan\theta = m/n$, with $m = 3$ and $n = 5$.

As shown by the solid lines in Fig. 3, the situation is totally different for the bounceback condition when the flow is no longer parallel to a symmetry axis of the lattice ($\alpha' = x'$, $0° < \theta < 45°$). These results show that the bounceback condition leads to unphysical oscillations of the density, which should be constant, and the normal component of the momentum, which should be zero. Not only do similar oscillations appear on the tangential momentum, but also its average value is shifted. When these effects are compared for two different widths, one sees that they are located near the walls (boundary or Knudsen layer) and that their amplitudes are almost constant for the chosen normalization. This result shows that these errors scale like $1/h'$; then the simulations with the bounceback condition are only first-order accurate in the size of the domain. Thus, bounceback conditions cause the appearance of Knudsen-type nonhydrodynamic solution near an inclined wall. The principal reason for that is *local* mass conservation enforced by the bounceback condition. In fact, it can be analytically proven that the mass is not locally conserved for the solution (71) when a no-slip condition is correctly imposed and the channel is inclined with lattice links; a simplified proof is given in the next section for Couette flows.

3.4.2. Couette Flow in Inclined Channels. We consider stationary Couette flow in an inclined channel in order to demonstrate an application of the LSOB method to flows with a nonzero momentum on an obstacle. In fact, one of the advantages of the LSOB method in comparison with the classical reflections is that nonzero momentum can be introduced into the flow in the same manner as zero momentum.

Let the flow be parallel to the x axis; as above, the z axis is perpendicular to the solid walls [see (60)] and h' is the width of the channel. The velocity of the lower wall is equal to u_0 and the upper one is immobile. Thus, the stationary Couette solution is

$$u_{x'} = u_0 \left(1 - \frac{z'}{h'}\right), \qquad 0 \leqslant z' \leqslant h', \quad \rho = \rho_0 \tag{73}$$

The exact solution of the lattice Boltzmann equation (1) for this linear flow becomes [see (72)]

$$N_i(\mathbf{r}) = d + d' \left[j_{x'}(\mathbf{r})\, C_{ix'} + \frac{1}{\lambda_\psi} \frac{\partial j_{x'}}{\partial z'} Q_{ix'z'} \right], \qquad \rho = \rho_0 \tag{74}$$

When a combination of bounceback and specular reflections is applied, a first-order analysis gives an exact location of the immobile wall in the linear flows, provided that the channel is not inclined (see ref. 14 for FHP,

ref. 17 for FCHC). In particular, the no-slip condition is satisfied exactly in the middle between the last nodes in the fluid and the next solid ones, when "pure" bounceback reflection is implemented. However, one observes at the boundary nodes near the immobile wall of an inclined channel that the velocity perpendicular to it does not vanish when bounceback reflection is applied, in a way similar to the Poiseuille flow shown Fig. 3. Hence, the exact solution (73) cannot be obtained in inclined channels by the lattice Boltzmann method with bounceback condition. Again the problem is linked to the local conservation of mass. The difference between the LSOB and bounceback methods is easily checked for Couette flows in the x' direction and a node r_5. For these nodes there is only one incoming and one outgoing population respectively, with velocities $\mathbf{C}_{18}$ and $\mathbf{C}_4$ [see (67)]. Using (74) and the fact that $\partial j_{x'}/\partial z'$ is constant for Couette flows, the mass flux on the nodes r_5 is given for the fixed wall by

$$N_4^{\text{out}} - N_{18}^{\text{in}} = d' C_{4x'}(C_{4z'} + 2\,\delta(\mathbf{z}_0))\,\frac{\partial j_{x'}}{\partial z'} \tag{75}$$

with $C_{4x'} = \sin\theta - \cos\theta$ and $C_{4z'} = \sin\theta + \cos\theta$. Obviously this mass flux is in general nonzero for $0° < 0 < 45°$ and cannot satisfy the bounceback condition $N_{18}^{\text{in}} = N_4^{\text{out}}$.

To simulate exactly Couette flows, one can. apply the LSOB method in its general 3D or 2D form with $j_{x'}^{\text{sol}}(\mathbf{z}_0)$ equal to $\rho_0 u_0$ (resp. zero) for the boundary nodes near the mobile (resp. immobile) wall. However, since the flow is linear, only one derivative a zl is required to compute exactly the unknown populations. This is discussed in some more detail in Appendix A.

4. CONCLUSION

A general approach to boundary conditions in lattice Boltzmann models has been described. This approach is based on a second-order Chapman–Enskog expansion of the populations. An explicit boundary method was then developed in order to introduce arbitrarily inclined, flat solid walls with a third-order error. The distance δ between lattice nodes and the modeled solid wall is adjustable, provided that stability conditions are satisfied. The resulting solution for the unknown populations at boundary nodes is expressed in the form of a linear combination of the known populations, supplied locally by the lattice Boltzmann equation. From the point of view of numerical efficiency and adaptation to parallel calculations, the method is not essentially different from standard, implicit boundary conditions.

This technique reduces the effects of the nonhydrodynamic modes near solid boundaries caused by local or almost local mass conservation inherent to classical reflections. It allows exact simulations of stationary flows, with a constant-curvature profile, in arbitrarily inclined channels with moving or immobile walls (e.g., Poiseuille and Couette flows between two plates). The second-order boundary algorithms developed earlier for solid walls parallel with some lattice links represent very particular cases of the LSOB method.

The generalization of this boundary technique to smoothly curved walls is currently under study. Some preliminary results have been obtained for a generalization of the method to circular solid walls and have shown that flows in arbitrarily small elliptic pipes can be simulated *exactly* these results will be reported elsewhere.

Besides other straightforward extensions of this method, for instance to multivelocity lattice Boltzmann models or solid walls arbitrarily inclined with respect to the lattice, several difficult problems remain. The first one is related to the different techniques to implement the method; although they give the same solution for Couette or Poiseuille flows, this will no longer be true for general flows with higher order derivatives. The effects of the different algorithms on the quality and the stability of the numerical scheme require further investigations. Finally, geometries with sharp edges are quite common in engineering applications and it would be important to extend the present approach to such boundaries. For this last problem, two difficulties remain. The first one is to find an appropriate method to match the constraints on the two walls. The second difficulty is to specify the effective accuracy order when some derivatives of the velocity field are not defined on the sharp edges. Despite these difficulties, preliminary simulations of flows in square pipes have shown that the LSOB method is more accurate than the bounceback rule.

APPENDIX A. POISEUILLE AND COUETTE FLOWS

A.1. Other Form of LSOB Method

In this appendix, we first describe an alternative way to construct second-order boundary conditions in lattice Boltzmann models. In this case, the Dirichlet condition is approximated as

$$J_{\alpha'}(\mathbf{z}_0) = j_{\alpha'}^{\text{sol}} + \delta \frac{\partial j_{\alpha'}}{\partial z'}(\mathbf{z}_0) - \frac{1}{2}\delta^2 \frac{\partial^2 j_{\alpha'}}{\partial z'^2}(\mathbf{z}_0) + O(\varepsilon^3), \qquad \alpha' = \{x', y', z'\} \quad \text{(A.1)}$$

The next step relates the derivatives in (A.1) to the coefficients (31) and (39) of the Chapman–Enskog expansion. Using (22), one can easily show,

at least for flows near a flat wall, that the derivatives in (A.1) can be represented as linear combinations of the coefficients (31) and (39). This becomes especially simple for Poiseuille flows, for which (72) can be written

$$N_i(\mathbf{r}) = d(\mathbf{r}) + d' j_{\alpha'}(\mathbf{r})\, C_{i\alpha'} + E_{\alpha' z'}(\mathbf{r})\, Q_{i\alpha' z'} + E_{\alpha' z' z'}(\mathbf{r})\, T_{i\alpha' z' z'} \qquad \alpha' = x' \quad \text{or} \quad \alpha' = y \tag{A.2}$$

where

$$E_{\alpha' z'}(\mathbf{r}) = \frac{d'}{\lambda_\psi} \frac{\partial j_{\alpha'}}{\partial z'}(\mathbf{r}) \tag{A.3}$$

$$E_{\alpha' z' z'} = d' \frac{\nu}{\lambda_2} \frac{\partial^2 j_{\alpha'}}{\partial z'^2} \tag{A.4}$$

The vector $\mathbf{T}_{\alpha' z' z'}$ is obtained by rotation of $\mathbf{T}_{\alpha z z}$ as done previously for the vectors $\mathbf{Q}_{\alpha' \beta'}$, and $\mathbf{Q}_{\alpha\beta}$ in Section 2:

$$T_{i\alpha' z' z'} = C_{i\alpha'} - \frac{D+2}{c^2} C_{i\alpha'} C_{iz'}^2 \tag{A.5}$$

Then, substituting the Taylor approximation (A.1) in (A.2), we have

$$N_i(\mathbf{z}_0) = d + d' j_{\alpha'}^{\text{sol}} C_{i\alpha'} + \mathbf{X}(\mathbf{z}_0) \cdot \mathbf{e}_i(\mathbf{z}_0) \tag{A.6}$$

with

$$\mathbf{X}(\mathbf{z}_0) = \{E_{\alpha' z'}, E_{\alpha' z' z'}\}(\mathbf{z}_0) \tag{A.7}$$

$$\mathbf{e}_i(\mathbf{z}_0) = \{e_{i\alpha' z'}, e_{i\alpha' z' z'}\} \tag{A.8}$$

and

$$\begin{aligned} e_{i\alpha' z'} &= Q_{i\alpha' z'} + p_1 C_{i\alpha'} \\ e_{i\alpha' z' z'} &= T_{i\alpha' z' z'} - p_2 C_{i\alpha'} \end{aligned} \tag{A.9}$$

The local parameters p_1 and p_2 are related to the distance δ between $\mathbf{z}_0$ and the wall by

$$\begin{aligned} p_1 &= \lambda_\psi \delta \\ p_2 &= \frac{\lambda_2}{2\nu} \delta^2 \end{aligned} \tag{A.10}$$

Note that if

$$\sum_{i \in I^{\text{in}}(\mathbf{z}_0)} \mathbf{e}_i = 0 \tag{A.11}$$

for instance when $\alpha' = x(\theta = 0°)$ or $\alpha' = y$, then we have [cf. (51)]

$$\sum_{i \in I^{\text{in}}(\mathbf{z}_0)} P_{ij} = 0 \tag{A.12}$$

and

$$\sum_{j \in I^{\text{use}}(\mathbf{z}_0)} \sum_{i \in I^{\text{in}}(\mathbf{z}_0)} P_{ij} = 0 \tag{A.13}$$

Hence, when the condition (A.11) is satisfied, the matrix $\mathbf{P}^{\text{use}}$ coincides with the matrix $\mathbf{P}$ [cf. (57)]. In addition, when (A.11) is true and $\mathbf{j}^{\text{sol}} = 0$ or $\sum_{k \in I^{\text{in}}(\mathbf{z}_0)} \mathbf{C}_k = 0$, the local density in (54) becomes equal to the mean density of the known populations N_i^{loc}.

Thus, in the 1D case (A.6)–(A.9), $\mathbf{X}$ can be computed at each boundary node from only two known populations such that the corresponding $\det[\mathbf{e}^{\text{use}}]$ is nonzero. If the known populations N_1^{loc} and N_2^{loc} (see Fig. 2a) are chosen for N_1^{use} and N_2^{use}, the $[2 \times 2]$ matrix $\mathbf{e}^{\text{use}}$ becomes [cf. (A.8)–(A.9)

$$\mathbf{e}^{\text{use}} = \begin{pmatrix} Q_{1\alpha'z'} + p_1 C_{1\alpha'} & T_{1\alpha'z'z'} - p_2 C_{1\alpha'} \\ Q_{2\alpha'z'} + p_1 C_{2\alpha'} & T_{2\alpha'z'z'} - p^2 C_{2\alpha'} \end{pmatrix} \tag{A.14}$$

In Appendix B a linear stability analysis shows that the lattice Boltzmann equation with the LSOB condition is expected to be stable when the solid wall is located outside the lattice ($\delta \leqslant 0$). With this condition, the sign of the parameters p_1 and p_2 is also determined because the eigenvalues of the collision matrix should be in the interval $]-2, 0[$ to satisfy the linear stability conditions.[2] Consequently, the study of $\det[\mathbf{e}^{\text{use}}]$ can be limited to the following intervals:

$$p_1 \geqslant 0, \qquad p_2 \leqslant 0 \tag{A.15}$$

Note also that the populations for a Couette flow are also given by (A.6) with $E_{\alpha'z'z'} = 0$. Hence, in order to simulate exactly this flow, it is enough to derive the value of tbe coeficient $E_{x'z'}$ from some known population N_i^{loc} or N_i^{out} provided $e_{ix'z'} \neq 0$.

A.1.1. Example: Poiseuille Flow in a Noninclined Channel. Our goal is to enforce no-slip walls at a chosen distance, equal to $-\delta$, from

the last upper and lower boundary nodes. In this case, all the boundary nodes are of the same type, labeled r_3 in (68) (see also Fig. 2a). In order to obtain $\det[\mathbf{e}^{use}] \neq 0$ in (A.14), N_1^{loc} and N_2^{loc} must be chosen such that

$$C_{1z} \neq C_{2z}, \qquad C_{1\alpha'} \neq 0, \qquad C_{2\alpha'} \neq 0 \qquad \text{with} \quad \alpha' = x \quad \text{or} \quad \alpha' = y \tag{A.16}$$

For instance, for the boundary nodes $\mathbf{z}_0$ near the upper wall, one can take

$$\begin{aligned} C_{1z} &= 1, \qquad C_{1\alpha'} = 1 \\ C_{2z} &= 0, \qquad C_{2\alpha'} = 1 \end{aligned} \tag{A.17}$$

with the corresponding matrix $\mathbf{e}^{use}$ in (A.14) given by

$$\mathbf{e}^{use} = \begin{pmatrix} 1+p_1 & -2-p_2 \\ p_1 & 1-p_2 \end{pmatrix}, \qquad \det[\mathbf{e}^{use}] = 1 + 3p_1 - p_2 \tag{A.18}$$

Thus, $\det[\mathbf{e}^{use}]$ is nonzero for any parameters p_1, p_2 which satisfy the conditions (A.15). For Poiseuille flows, the vector $\mathbf{e}_i$ is proportional to $C_{i\alpha'}$ [cf. (A.8)–(A.9)]. Consequently, the conditions (A.11)–(A.13) are satisfied in noninclined channel due to symmetry and the local density d is equal to the mean value of the known local populations N_i^{loc} [see (54)]. Note also that the mass is locally conserved in noninclined channels since the sum of populations N_i^{out} is equal to the sum of unknown populations N_i^{in} due to symmetry. Thus, only the matrix $\mathbf{P}$ of (51) must be found in order to impose no-slip walls in a noninclined Poiseuille flow. For instance, when the no-slip walls are implemented exactly on the last lattice nodes ($\delta = 0$), both parameters p_1 and p_2 are equal to zero [cf. (A.10)]. Consequently, the solution (51) with (A.8), (A.9), and (A.18) gives

$$\begin{aligned} N_\perp^{in} &\equiv d, & C_{\perp\alpha'} &= 0 \\ N_\beta^{in} &= 6d - \{N^{loc} + 4N_2^{loc}\}, & C_{\beta z} &= -1, \quad C_{\beta\alpha'} = 1 \\ N_\gamma^{in} &= -4d + \{N_1^{loc} + 4N_2^{loc}\}, & C_{\gamma z} &= -1, \quad C_{\gamma\alpha'} = -1 \end{aligned} \tag{A.19}$$

Note that the solution (A.19) is not the only one. One could use any other pair of known populations N_i^{loc} or any pair of populations N_i^{out} which satisfy the conditions (A.16). One can also determine N_j^{use} as a more general linear combination of the populations N_i^{loc} and (or) N_i^{out}. For this particular flow, one can also represent the unknown populations as a linear combination of N_{-1}^{loc} and N_{-2}^{loc} (or) N_{-1}^{out} and N_{-2}^{out} which do not satisfy the conditions (A.16) since $C_{-1z'} = C_{-2z'}$ (see Fig. 2a). In such a case, $\det[\mathbf{e}^{use}]$ given in (A.18) is equal to zero and hence one cannot derive

both first- and second-order derivatives (A.7) from these populations. Nevertheless, using the relation between these derivatives for the Poiseuille equation (71), one can find a solution in the form of a linear combination of such populations. In particular, when N_{-1}^{out} and N_{-2}^{out} are used, one obtains the solution for the proportion p in combination of bounceback and specular reflections

$$\begin{aligned} N_{\beta}^{\text{in}} &= pN_{-1}^{\text{out}} + (1-p)\, N_{-2}^{\text{out}} \\ N_{\gamma}^{\text{in}} &= (1-p)\, N_{-1}^{\text{out}} + pN_{-2}^{\text{out}} \end{aligned} \tag{A.20}$$

This kind of solution for noninclined channels and for channels inclined at 45° with FCHC lattice links has been already discussed in ref. 17. It is worth mentioning however, that the solution for p depends not only on the distance δ, but also on the width of the computational domain while the matrix $\mathbf{P}$ does not depend upon it.

A.2. Conservation of Total Mass by LSOB Method for Couette and Poiseuille Flows

As predicted from general arguments in Section 2.6, our numerical simulations confirm that the LSOB method conserves the total mass automatically in stationary Couette and Poiseuille flows. Indeed this result should hold analytically and we are going to show this below when $\tan\theta$ is a rational number m/n, with n and m relatively prime and $2 \leqslant m < n$, and for the simplified discretization of the solid wall illustrated in Fig. 4. This discretization is rougher than the "stair-type" one shown in Fig. 2b; however, it is easier to manipulate analytically since the distribution of boundary nodes is given for $2 \leqslant m < n$ by the periodic replication of the following pattern:

$$(r_4^{\perp}, \overbrace{r_3^{\perp},\ldots, r_3^{\perp}}^{(m-2)\text{ times}}, r_0, \overbrace{r_3,\ldots, r_3}^{(n-2)\text{ times}}, r_4, r_5) \tag{A.21}$$

where the pseudo-2D-corner r_0 is described using the notations (68) by

$$\text{node } r_0\text{:} \qquad L^+ = 9, \qquad L^- = 9, \qquad I^{\text{loc}} = \{3,\ldots, 9, 11, 12\} \tag{A.22}$$

and $r_3^{\perp}$ (resp. $r_4^{\perp}$) is derived from r_3 (resp. r_4) through the symmetry with respect to the plane $x + z = 0$.

The mass flux through a given wall is zero if the sum of unknown populations entering the lattice along this wall is equal to the sum of populations leaving the lattice through if:

$$\sum_{\mathbf{z}_0} \sum_{i \in I^{\text{in}}(\mathbf{z}_0)} N_i^{\text{in}}(\mathbf{z}_0) = \sum_{\mathbf{z}_0} \sum_{i \in I^{\text{out}}(\mathbf{z}_0)} N_i^{\text{out}}(\mathbf{z}_0) \tag{A.23}$$

With the help of the Boltzmann equation (1), the populations $N_i^{\text{out}}(\mathbf{z}_0)$ can be easily derived from the populations $N_i(\mathbf{z}_0)$ in (A.2) as

$$N_i^{\text{out}}(\mathbf{z}_0) = N_i(\mathbf{z}_0) + d'\rho \mathbf{F} \cdot \mathbf{C}_i + \lambda_\psi E_{\alpha' z'} + \lambda_2 E_{\alpha' z' z'} T_{i\alpha' z' z'}, \qquad i \in I^{\text{out}} \tag{A.24}$$

where $E_{\alpha' z' z'}$, and $\mathbf{F}$ are identically zero for Couette flows.

When (A.2) and (A.24) are substituted into (A.23), the conservation of the total mass in Couette flow implies that the following must be satisfied:

$$\sum_{\mathbf{z}_0} \sum_{i \in I^{\text{in}}(\mathbf{z}_0)} C_{i\alpha'} \equiv 0 \tag{A.25}$$

$$\sum_{\mathbf{z}_0} \sum_{i \in I^{\text{in}}(\mathbf{z}_0)} [-C_{i\alpha'} C_{iz'} + 2\delta(\mathbf{z}_0)\, C_{i\alpha'}] \equiv 0 \tag{A.26}$$

for $\alpha' = x'$ and $\alpha' = y$. Note that, when (A.25) is satisfied, (A.26) is left unchanged by the addition of an arbitrary distance to $\delta(\mathbf{z}_0)$.

One can easily verify for "rough" discretization that the relation (A.25) is satisfied for any angle θ. In order to verify (A.26), let us calculate $\delta(\mathbf{z}_0)$ for each boundary node $\mathbf{z}_0$ obtained from the "rough" discretization. Let $(k=1,\ j=1)$ correspond to the boundary node r_0 (see Fig. 4). Then for horizontal boundary nodes $k(k=1,\ldots, n)$ and for vertical boundary nodes $j(j=2,\ldots, m+1)$, $\delta(\mathbf{z}_0)$ is given by

$$\begin{aligned} \delta(k, 1) &= \delta(1, 1) - (k-1)\sin\theta, \qquad k \in \{1,\ldots, m\} \\ \delta(1, j) &= \delta(1, 1) - (j-1)\cos\theta, \qquad j \in \{2,\ldots, m+1\} \end{aligned} \tag{A.27}$$

Then, using (A.25), the relation (A.26) becomes

$$\begin{aligned} &\sum_{\mathbf{z}_0} \sum_{i \in I^{\text{in}}(\mathbf{z}_0)} C_{i\alpha'} + 2\sin\theta \sum_{k=2}^{n} (k-1) \sum_{i \in I^{\text{in}}(k,1)} C_{i\alpha'} \\ &\quad + 2\cos\theta \sum_{j=2}^{m+1} (j-1) \sum_{i \in I^{\text{in}}(1,j)} C_{i\alpha'} \equiv 0 \end{aligned} \tag{A.28}$$

One can verify that the relation (A.28) is satisfied for any angle θ.

In addition to the relations (A.25)–(A.26) derived for Couette flow, the conservation of total mass (A.23) imposes two additional constraints for Poiseuille flows:

$$\sum_{\mathbf{z}_0} \sum_{i \in I^{\text{in}}(\mathbf{z}_0)} T_{i\alpha' z' z'} \equiv 0 \tag{A.29}$$

and

$$\sum_{\mathbf{z}_0} \sum_{i \in I^{\text{in}}(\mathbf{z}_0)} [-\delta(\mathbf{z}_0)\, C_{i\alpha'} C_{iz'} + \delta^2(\mathbf{z}_0)\, C_{i\alpha'}] \equiv 0 \tag{A.30}$$

where (A.30) have been obtained with the help of (22) and $\partial j'_\alpha / \partial z'$ constant on the wall. Note also that (A.30) is left unchanged by the addition of an arbitrary distance to $\delta(\mathbf{z}_0)$ when (A.25) and (A.26) are satisfied.

In "rough" discretization, one can easily verify that the relation (A.29) is satisfied for any angle θ. With the help of (A.25) and (A.26), the substitution of the relation (A.27) in (A.30) yields

$$\begin{aligned} \sin\theta \sum_{k=2}^{n} (k-1) \sum_{i \in I^{\text{in}}(\mathbf{z}_0)} C_{i\alpha'} C_{iz'} + \cos\theta \sum_{j=2}^{m+1} (j-1) \sum_{i \in I^{\text{in}}(\mathbf{z}_0)} \\ + \sin^2\theta \sum_{k=2}^{2} (k-1)^2 \sum_{i \in I^{\text{in}}(\mathbf{z}_0)} C_{i\alpha'} + \cos^2\theta \sum_{j=2}^{m+1} (j-1)^2 \sum_{i \in I^{\text{in}}(\mathbf{z}_0)} C_{i\alpha'} \equiv 0 \end{aligned} \tag{A.31}$$

As above, this relation can be easily verified for "rough" discretization.

It is easy to check that these relations hold for $(m, n) = (1, 1)$ and $m = 1$ and $n \geqslant 2$. We conjecture that they hold for any discretization of a plane with a rational inclination, although the full proof seems quite technical.

APPENDIX B. SIMPLIFIED LINEAR STABILITY ANALYSIS OF THE LSOB METHOD

Neglecting the nonlinear terms in the equilibrium distribution, a linear stability analysis of the lattice Boltzmann methods has been performed for uniform flows.[2, 26] Von Neumann linearized stability analysis is given in ref. 27. Nevertheless, the influence of boundary conditions on the stability conditions is not considered in these works. However, this question should be raised even for standard bounceback and specular reflections.

In this section, we first write the evolution equation for the lattice Boltzmann equation with linear boundary conditions in which the

unknown populations $N_i^{\text{in}}(\mathbf{z}_0)$ are expressed as linear combinations of the populations $N_i^{\text{loc}}(\mathbf{z}_0)$ and $N_i^{\text{out}}(\mathbf{z}_0)$, Then we study the zero-wavenumber stability of this scheme, assuming a stationary flow parallel to the x axis of a FHP lattice and invariant by translation along the solid wall. The FHP model is chosen in order to decrease the dimension of the resulting evolution matrix. We neglect nonlinear terms in the equilibrium solution (6) as always in this paper.

Thus, the evolution equation (1) with the considered boundary conditions can be written

$$\mathbf{N}(\mathbf{r}, t+1) = \mathscr{P}(\mathbf{r}) \cdot \mathscr{S} \cdot \mathbf{N}^*(\mathbf{r}, t) \tag{B.1}$$

where the $2b_m$ elements of $\mathbf{N}^*(\mathbf{r}, t)$ are the population at the node $\mathbf{r}$ and the neighboring ones

$$\mathbf{N}^*(\mathbf{r}, t) = \{\mathbf{N}(\mathbf{r}, t), (N_i(\mathbf{r} - \mathbf{C}_i, t), \in \{1, ..., b_m\})\} \tag{B.2}$$

$\mathscr{S}$ is the diagonal matrix consisting of two equal blocks, each block being the sum of the identity matrix $\mathscr{I}$ and the collision matrix $\mathscr{A}$

$$\mathscr{S} = \begin{pmatrix} \mathscr{I} + \mathscr{A} & \\ & \mathscr{I} + \mathscr{A} \end{pmatrix} \tag{B.3}$$

and the $[b_m \times 2b_m]$ matrix $\mathscr{P}(\mathbf{r})$ includes the boundary conditions in the evolution equation

$$\mathscr{P}_{ij}(\mathbf{r}) = \begin{cases} \delta_{ik}, \quad k = j - b_m, & \text{if} \quad i \in I^{\text{loc}}(\mathbf{r}), \quad j \in \{1, ..., 2b_m\} \\ \tilde{P}_{ij}(\mathbf{r}) & \text{if} \quad i \in I^{\text{in}}(\mathbf{r}), \quad j \in \{1, ..., 2b_m\} \end{cases} \tag{B.4}$$

where $\tilde{\mathsf{P}}(\mathbf{r})$ is any matrix of local boundary conditions at the node $\mathbf{r}$, similar to the one given by (57).

When zero-wavenumber perturbations are considered the stability conditions are given by the eigenvalues of the evolution matrix $\mathscr{P}(\mathbf{r}) \cdot \mathscr{S}$. Let us give here such an analysis for a system of minimal size. Assuming the flow invariant by translation along the x-axis of the FHP lattice and periodic boundary conditions along this axis, it is enough to consider only one node in this direction. In the perpendicular y direction, the system is limited by two solid walls parallel to the x axis and consists of only two lattice nodes y_1 and y_2 (see Fig. 5).

The six populations $N_i(\mathbf{r}, t)$ corresponding to the FHP velocities are nubered the usual way,

$$\mathbf{C}_i = \{\cos[(i-1)\,\pi/3], \sin[(i-1)\,\pi/3]\}, \qquad i \in \{1, ..., b_m\}, \quad b_m = 6 \tag{B.5}$$

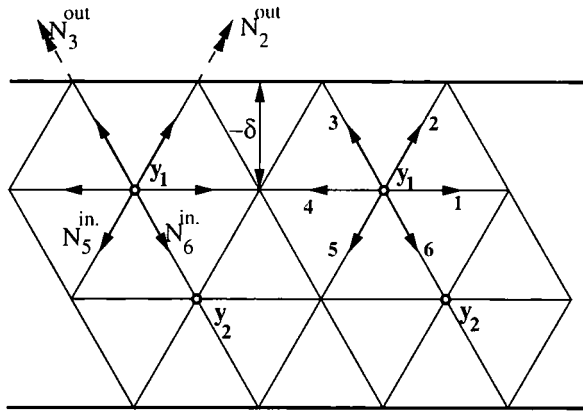

Fig. 5. Simplified geometry for linear stability analysis on the FHP lattice.

Hence, the entire system is described by the 12 populations $\mathbf{N}_i(y_1, t)$ and $\mathbf{N}_i(y_2, t)$ with two unknown and four known populations on each node (see Fig.5). The evolution of the whole system is described by

$$\mathbf{N}^*(t+1) = \mathscr{P} \cdot \mathscr{S} \cdot \mathbf{N}^*(t), \qquad \mathbf{N}^*(t) = \{\mathbf{N}(y_1, t), \mathbf{N}(y_2, t)\} \tag{B.6}$$

where $\mathbf{N}^*(t)$ denotes the concatenation of $\mathbf{N}^*(y_1, t)$ and $\mathbf{N}^*(y_2, t)$, and $\mathscr{P}$ is the $[2b_m \times 2b_m]$ matrix obtained from $\mathscr{P}(y_1)$, $\mathscr{P}(y_2)$, and periodic boundary conditions. In order to conserve the mass along each wall and due to symmetry, it can be written in the following general form:

$$\mathscr{P} = \begin{bmatrix}
1 & 0 & 0 & 0 & 0 & 0 & 0 & 0 & 0 & 0 & 0 & 0 \\
0 & 0 & 0 & 0 & 0 & 0 & 0 & 1 & 0 & 0 & 0 & 0 \\
0 & 0 & 0 & 0 & 0 & 0 & 0 & 0 & 1 & 0 & 0 & 0 \\
0 & 0 & 0 & 1 & 0 & 0 & 0 & 0 & 0 & 0 & 0 & 0 \\
w_1 & p & 1-p & -w_0 & 0 & 0 & 0 & w_2 & -w_2 & 0 & 0 & 0 \\
-w_1 & 1-p & p & w_1 & 0 & 0 & 0 & -w_2 & w_2 & 0 & 0 & 0 \\
0 & 0 & 0 & 0 & 0 & 0 & 1 & 0 & 0 & 0 & 0 & 0 \\
0 & 0 & 0 & 0 & w_2 & -w_2 & w_1 & 0 & 0 & -w_1 & p & 1-p \\
0 & 0 & 0 & 0 & -w_2 & w_2 & -w_1 & 0 & 0 & w_1 & 1-p & p \\
0 & 0 & 0 & 0 & 0 & 0 & 0 & 0 & 0 & 1 & 0 & 0 \\
0 & 0 & 0 & 0 & 1 & 0 & 0 & 0 & 0 & 0 & 0 & 0 \\
0 & 0 & 0 & 0 & 0 & 1 & 0 & 0 & 0 & 0 & 0 & 0
\end{bmatrix} \tag{B.7}$$

where the parameters w_1, w_2, p are derived from the matrices of boundary conditions $\mathsf{P}(y_1)$ and $\mathsf{P}(y_2)$ in (B.4). For instance, $p \equiv 1$, $w_1 = 0$, $w_2 = 0$ corresponds to the bounceback condition, and $w_= 0$, $w_2 = 0$ to a Combination of bounceback and specular reflections with the proportions p and $1-p$.

Since the matrices $\mathscr{P}$ and $\mathscr{S}$ are real, sufficient stability conditions for Eq. (B.6) are obtained when all the eigenvalues of the matrices $\mathscr{P}^t \cdot \mathscr{P}$ and $\mathscr{S}^t \cdot \mathscr{S}$ have a modulus less than unity. For the matrix $\mathscr{S}$. such conditions are fulfilled when the eigenvalues of the collision matrix $\mathscr{A}$ are in the interval $]-2, 0[$

$$-2 < \lambda_\psi < 0, \qquad -2 < \lambda_2 < 0 \tag{B.8}$$

as predicted by the linear analysis (2) of lattice Boltzmann models. The analysis of the matrix $\mathscr{P}^t\mathscr{P}$ shows that sufficient stability conditions are

$$0 \leqslant p \leqslant 1, \qquad w_1 \equiv 0, \qquad w_2 \equiv 0 \tag{B.9}$$

i.e., a combination of bounceback and specular reflections with the proportion p between zero and one.

However, one can try to extend the interval of stability by analyzing the whole evolution operator $\mathscr{P} \cdot \mathscr{S}$. The scheme would be stable provided that the eigenvalues of the matrix $(\mathscr{P} \cdot \mathscr{S})^t (\mathscr{P} \cdot \mathscr{S})$ have a modulus less than unity. One can show that in the general case (B.7) it is enough to study the eigenvalues of the matrix $\mathscr{P} \cdot \mathscr{S}$ to derive the stability conditions. For this purpose, we represent the matrix $\mathscr{P} \cdot \mathscr{S}$ in the physical basis $\{\mathbf{s}_1, ..., \mathbf{s}_{12}\}$, expressed in terms of the eigenvectors $\{\mathbf{n}_1, ..., \mathbf{n}_6\}$ of the collision operator $\mathscr{A}$ as

$$\mathbf{s}_i = \{\mathbf{n}_i, \mathbf{n}_i\}, \qquad \mathbf{s}_{i+6} = \{\mathbf{n}_i, -\mathbf{n}_i\}, \qquad i \in \{1, ..., 6\} \tag{B.10}$$

where the eigenvectors of FHP collision operator $\mathscr{A}$ can be given as[14, 23]

$$\begin{aligned} &\mathbf{n}_1 = \{1, 1, 1, 1, 1, 1\}, \qquad \mathbf{n}_2 = \mathbf{C}_x, \qquad \mathbf{n}_3 = \mathbf{C}_y \\ &\mathbf{n}_4 = \mathbf{Q}_{xx} = -\mathbf{Q}_{yy}, \qquad \mathbf{n}_5 = \mathbf{Q}_{xy}, \qquad \mathbf{n}_6 = \mathbf{T}_{xyy} \end{aligned} \tag{B.11}$$

In the physical basis (B.10)–(B.11), the matrix $\mathscr{S}$ is diagonal, with diagonal elements

$$\{1, 1, 1, 1+\lambda_\psi, 1+\lambda_\psi, 1+\lambda_2, 1, 1, 1, 1+\lambda_\psi, 1+\lambda_\psi, 1+\lambda_2\}$$

Expressing $\mathscr{P}$ in the physical basis, we can abtain the characteristic polynomial $\chi(\lambda)$ of the $\mathscr{P} \cdot \mathscr{S}$ as a function of the parameters $p, w_1, w_2, \lambda_\psi, \lambda_2$. When the sum of populations leaving the lattice is distributed equally

between the two unknown populations, the parameter p is equal to 1/2. For the sake of simplicity, the subsequent analysis is done for the so-called *single-time relaxation*[28, 29] or BGK method[30] only:

$$\lambda_\psi = \lambda_2 = \tau \tag{B.12}$$

Under these conditions, the characteristic polynomial has the following form

$$\chi(\lambda) = \lambda^2(1+\tau-\lambda)(\lambda^2-1)\,\chi_1(\lambda,\tau)\,\chi_2(\lambda,\tau,w_1,w_2)\,\chi_3(\lambda,\tau,w_1,w_2) \tag{B.13}$$

where the polynomials χ_1, χ_2 and χ_3 are given by

$$\begin{aligned}
\chi_1(\lambda,\tau) &= 3(1+\tau)(1-\lambda)+(3+2\tau)\,\lambda^2-3\lambda^3\\
\chi_2(\lambda,\tau,w_1,w_2) &= \chi_{21}+\chi_{22}\lambda+\chi_{23}\lambda^2\\
\chi_{21} &= -\tfrac{1}{2}(\tau+\tau^2)-w_1(6+7\tau+\tau^2)-2w_2(\tau+\tau^2)\\
\chi_{22} &= -3-\tfrac{1}{2}\tau+w_1(6+5\tau)-2w_2\tau\\
\chi_{23} &= 3\\
\chi_3(\lambda,\tau,w_1,w_2) &= \chi_{31}+\chi_{32}\lambda+\chi_{33}\lambda^2\\
\chi_{31} &= -\chi_{21}\\
\chi_{32} &= -3(1+\tfrac{1}{2}\tau)-w_1(6+5\tau)-2w_2\tau\\
\chi_{33} &= 3
\end{aligned} \tag{B.14}$$

Under the conditions (B.8), the roots of the equation $\chi_1(\lambda,\tau)=0$ have a modulus less than or equal to one. The roots of $\chi_2(\lambda,\tau,w_1,w_2)=0$ and $\chi_3(\lambda,\tau,w_1,w_2)=0$ are functions of the parameters w_1 and w_2 given by the LSOB method.

For flows parallel to a noninclined solid wall and invariant along it, the second-order populations is given by (A.6)–(A.9). For these flows the mass is locally conserved and the local density is automatically determined when the sum of the populations leaving the lattice is equally distributed between the two unknown populations at the boundary node ($p=1/2$).

Following the solution (A.6)–(A.9), two populations, $N_1^{\text{use}}(y)$ and $N_2^{\text{use}}(y)$ should be chosen in each boundary node in order to determine the solution for unknown populations. In order to obtain the matrix $\mathscr{P}$ in the symmetric form (B.7), one can take at the node y_1, for example (see Fig. 5)

$$\begin{aligned}
N_1^{\text{use}}(y_1) &= \tfrac{1}{2}\{N_1^{\text{loc}}-N_4^{\text{loc}}\}\\
N_2^{\text{use}}(y_1) &= \tfrac{1}{2}\{N_2^{\text{loc}}-N_3^{\text{loc}}\}
\end{aligned} \tag{B.15}$$

Node y_2 can be considered by analogy. Then the matrix $\mathbf{e}^{\text{use}}(y_1)$, written in (A.14) for any inclined channel, takes the form

$$\mathbf{e}^{\text{use}}(y_1) = \begin{pmatrix} Q_{1xy} + p_1 C_{1x} & T_{1xyy} - p_2 C_{1x} \\ Q_{2xy} + p_1 C_{2x} & T_{2xyy} - p_2 C_{2x} \end{pmatrix} \tag{B.16}$$

where the indices 1 and 2 for C_{ix}, Q_{ixy}, and T_{ixyy} correspond respectively to the populations N_1^{use} and N_2^{use} in (B.15). Only a $[2\times 2]$ matrix $\mathsf{P}(y_1)$ has to be determined in order to construct $N_5^{\text{in}}(y_1)$ and $N_6^{\text{in}}(y_1)$. The coefficients of this matrix determine the coefficients w_1 and w_2 in (B.7),

$$\begin{aligned} w_1 &= \mathbf{e}_5 \cdot [\mathbf{e}^{\text{use}}(y_1)]_1^{-1} \\ w_2 &= \mathbf{e}_5 \cdot [\mathbf{e}^{\text{use}}(y_1)]_2^{-1} \end{aligned} \tag{B.17}$$

where $[\mathbf{e}^{\text{use}}]_j^{-1}$ denotes the jth, column of the matrix $[\mathbf{e}^{\text{use}}]^{-1}$. The relations (B.16) and (B.17) give the following values for the coefficients w_1 and w_2:

$$\begin{aligned} w_1 &= -\frac{\sqrt{3}}{4\mathscr{D}}(2+p_2) \\ w_2 &= -\frac{1}{4\mathscr{D}}\{\sqrt{3}\,(1-p_2) - 6p_1\} \end{aligned} \tag{B.18}$$

where $\mathscr{D}$ denotes $\det[\mathbf{e}^{\text{use}}]$

$$\mathscr{D} = -\tfrac{1}{4}\{\sqrt{3}\,(1-p_2) + 6p_1\} \tag{B.19}$$

Note the dependence of the coefficients w_1 and w_2 upon the eigenvalues λ_ψ, and λ_2 and the distance δ hidden in the parameters p_1 and p_2 [see (A.10)].

When the eigenvalues λ_ψ and λ_2 are equal and the solution (B.18) is substituted into $\chi_2(\lambda, \tau, w_1, w_2)$ and $\chi_3(\lambda, \tau, w_1, w_2)$, the roots of these polynomials are functions of the eigenvalue τ and the algebraic distance δ. The analytical solution of this problem is the following: when τ satisfies (B.8) and the solid wall is located exactly on the last lattice nodes ($\delta = 0$) or *outside* of the lattice ($\delta < 0$), the roots of $\chi_2(\tau, \delta)$ and $\chi_3(\tau, \delta)$ are found in the interval of the asymptotic stability $[-1, 1]$. This result seems rather natural, since a combination of bounceback and specular reflections locates the no-slip wall outside of the last boundary nodes, at least for $0 < p \leqslant 1$.

Note also that considering the full evolution matrix $\mathscr{P}\cdot\mathscr{S}$ for a combination of bounceback and specular reflections, the interval of stability for p can be extended as a function of the eigenvalues λ_ψ and λ_2. More

precisely, one can show that negative values of p are not stable in agreement with physical intuition, whereas the upper limit $p = 1$, given by sufficient stability conditions, can be extended. Let us also mention that by assuming a flow invariant along the wall, one can perform a similar stability analysis for the FCHC lattice.

ACKNOWLEDGMENTS

We thank L. Giraud, P. Lallemand, D. H. Rothman, and L. Wagner for useful discussions and critical readings of the manuscript.

REFERENCES

1 U. Frisch, D. d'Humières, B. Hasslacher, P. Lallemand, Y. Pomeau, and J.-P. Rivet, Lattice gas hydrodynamics in two and three dimensiones, *Complex Systems* **1**:649 (1987).
2. F. J. Higuera and J. Jimenez, Boltzmann approach to lattice gas simulations, *Europhys. Lett.* **9**:663 (1989).
3. S. Succi, E. Foti, and F. Higuera, The lattice Boltzmann equation: A new tool for computational fluid dynamics, *Physica D* **47**:219 (1991).
4. D. H. Rothman and S. Zaleski, Lattice-gas models of phase separation: Interfaces, phase transitions, and multiphase flow, *Rev. Mod. Phys.* **66**:1417 (1994).
5. R. Benzi, S. Succi, and M. Vergasola, The lattice Boltzmann equation: Theory and applications, *Phys. Rep.* **222**:145 (1992).
6. D. H. Rothman, Cellular-automaton fluids: A model for flow in porous media, *Geophysics* **53**:509 (1988).
7. A. Cancelliere, C. Chang, E. Foti, D. H. Rothmans and S. Succi, The permeability of random medium: Comparison of simulations with theory, *Phys. Fluids A* **2**:2085 (1990).
8. S. Chen, K. Diemer, G. D. Doolen, K. Eggert, C. Fu, S. Gutman, and B. J. Travis, Lattice gas automata for flow through porous media, *Physica D* **47**:72 (1991).
9. B. Ferréol and D. Rothman, Lattice-Boltzmann simulations of flow through Fontainebleau sandstone, *Transport Porous Media* (1995).
10. A. J. C. Ladd, M. E. Colvin, and D. Frenkel, Application of lattice-gas cellular automata to the Brownian motion of solids in suspensions, *Phys. Rev. Lett.* **60**:975 (1988).
11. A. J. C. Ladd and D. Frenkel, Dissipative hydrodynamic interactions via lattice-gas cellular automata, *Phys. Fluids A* **2**:1921 (1990).
12. A. J. C. Ladd, Numerical simulations of particulate suspensions via a discretized Boltzmann equation. Part 1. Theoretical foundation, *J. Fluid Mech.* **271**:285 (1994).
13. A. J. C. Ladd, Numerical simulations of particulate suspensions via a discretized Boltzmann equation. Part 2. Numerical result, *J. Fluid Mech.* **271**:311 (1994).
14. R. Cornubert, D. d'Humières, and D. Levermore, A Knudsen layer theory, *Physica D* **47**:241 (1991).
15. R. Cornubert and D. d'Humières, Flow past a symmetric backfacing-step using lattice Boltzmann equation, unpublished.
16. I. Ginzbourg and P. M. Adler, Boundary flow condition analysis for the three-dimensional lattice Bolzmann model, *J. Phys. II France* **4**:191 (1994).
17. I. Ginzbourg, boundary conditions problems in lattice gas methods for single and multiple phases, Ph.D. thesis University of Paris VI (1994).

18. D. P. Ziegler, Boundary conditions for lattice Boltzmann simultations, *J. Stat. Phys.* **71**:1171 (1993).
19. D. R. Noble, S. Chen, J. G. Georgiadis, and R. O. Buckius, A consistent hydrodynamic boundary condition for the lattice Boltzmann method, *Phys. Fluids A* **7**:203 (1995).
20. P. A. Skordos, Initial and boundary conditions for the lattice Boltzmann method, *Phys. Rev. E* **48**:4823 (1993).
21. C. Appert and D. d'Humières, Density profiles in a diphasic lattice gas model, *Phys. Rev. E* **51**:4335 (1995).
22. F. Higuera, S. Succi, and R. Benzi, Lattice gas dynamics with enhanced collisions, *Europhys. Lett.* **9**:345 (1989).
23. R. Cornubert, D. d'Humières, and D. Levermore, A Knudsen layer theory for lattice gases, unpublished.
24. I. Ginzbourg, L. Giraud, and D. d'Humières, Efficient lattice-Boltzmann calculations in porous media, in preparation.
25. H. Schlishting, *Boundary Layer Theory* (McGraw-Hill, New York, 1968).
26. D. W. Grunau, Lattice methods for modeling hydrodynamics, Ph.D. thesis, Colorado State University (1993).
27. J. D. Sterling and S. Chen, Stability analysis of lattice Boltzmann methods, *J. Comp. Phys.*, submitted.
28. S. Chen, H. Chen, D. Martinez, and W. H. Matthaeus, Lattice Boltztmann model for simulation of magnetohydrodynamics, *Phys. Rev. Lett.* **67**:3776 (1991).
29. H. Chen, S. Chen, and W. H. Matthaeus, Recovery of the Navier–Stokes equations using a lattice-gas Boltzmann method, *Phys. Rev. A* **45**:R5339 (1992).
30. Y. H. Qian, D. d'Humières, and P. Lallemand, Lattice BGK models for Navier–Stokes equation, *Europhys. Lett.* **17**:479 (1992).